Received: 27 October 2023 | Revised: 18 November 2023 | Accepted: 3 December 2023

DOI: 10.1002/bte2.20230061

REVIEW

BATTERY ENERGY Open Access WILEY

Flexible wearable energy storage devices: Materials, structures, and applications

Qi Zhang[1] | Xuan-Wen Gao[2] | Xiao Liu[1] | Jian-Jia Mu[2] | Qinfen Gu[3] | Zhaomeng Liu[2] | Wen-Bin Luo[2]

[1]Engineering Research Centre of Advanced Metal Composites Forming Technology and Equipment, Ministry of Education, Taiyuan University of Technology, Taiyuan, China

[2]Institute for Energy Electrochemistry and Urban Mines Metallurgy, School of Metallurgy, Northeastern University, Shenyang, China

[3]Australian Synchrotron (ANSTO), Victoria, Australia

Correspondence
Wen-Bin Luo, Institute for Energy Electrochemistry and Urban Mines Metallurgy, School of Metallurgy, Northeastern University, No. 11 Lane 3, Wenhua Rd, Shenyang, China.
Email: luowenbin@smm.neu.edu.cn

Funding information
Shanxi-Zheda Institute of Advanced Materials and Chemical Engineering Program, Grant/Award Number: 2022SX-TD021; National Natural Science Foundation of China, Grant/Award Numbers: 52272194, 32301542; Fundamental Research Program of Shanxi Province, Grant/Award Numbers: 20210302123109, 20210302124426; LiaoNing Revitalization Talents Program, Grant/Award Number: XLYC2007155

Abstract

Wearable electronics are expected to be light, durable, flexible, and comfortable. Many fibrous, planar, and tridimensional structures have been designed to realize flexible devices that can sustain geometrical deformations, such as bending, twisting, folding, and stretching normally under the premise of relatively good electrochemical performance and mechanical stability. As a flexible electrode for batteries or other devices, it possesses favorable mechanical strength and large specific capacity and preserves efficient ionic and electronic conductivity with a certain shape, structure, and function. To fulfill flexible energy-storage devices, much effort has been devoted to the design of structures and materials with mechanical characteristics. This review attempts to critically review the state of the art with respect to materials of electrodes and electrolyte, the device structure, and the corresponding fabrication techniques as well as applications of the flexible energy storage devices. Finally, the limitations of materials and preparation methods, the functions, and the working conditions of devices in the future were discussed and presented.

KEYWORDS
electrode, electronics, energy storage device, flexible, wearable device

1 | INTRODUCTION

Due to the tension of living under high pressure, light, portable, multifunctional goods have become increasingly important to make our lives easier. Portable electronics such as wireless sensors, roll-up displays, electronic skins, and flexible smartphones are light in weight and come in smaller sizes that can easily be carried around. To achieve complete and independent wearable devices, it is vital to develop flexible energy

Qi Zhang and Xuan-Wen Gao contributed equally to this work.

storage devices. New-generation flexible electronic devices require flexible and reliable power sources with high energy density, long cycle life, excellent rate capability, and compatible electrolytes and separators. Besides, safety and cost should also be considered in the practical application.[1–4] A flexible and lightweight energy storage system is robust under geometry deformation without compromising its performance.

As usual, the mechanical reliability of flexible energy storage devices includes electrical performance retention and deformation endurance. As a flexible electrode, it should possess favorable mechanical strength and large specific capacity. And the electrodes need to preserve efficient ionic and electronic conductivity during cycling. Much effort has been put toward the design of structures and materials with mechanical characteristics to realize flexible devices that can sustain geometrical deformations, such as bending, twisting, folding, and stretching (Figure 1).[5,6] In contrast with conventional electrodes, flexible electrodes are usually fabricated without a binder, a conductive additive, or even a current collector. Inspired by this, flexible energy storage systems such as flexible alkaline batteries,[7] flexible zinc carbon batteries,[8] all-polymer batteries,[9] flexible rechargeable ion batteries,[10,11] and flexible supercapacitors (SCs)[12] have been explored and investigated. Among these, flexible rechargeable batteries (e.g., lithium-ion batteries, sodium-ion batteries, and lithium-sulfur) are very promising.[13,14] They have shown performance limitations in their short cycle life, relatively slow charging–discharging rates, and lower power densities. To compensate for the lower power densities of these batteries, SCs, also known as electrochemical capacitors (ECs) or ultracapacitors, have emerged as considerable alternative candidates to batteries and offer a number of potential advantages in performance, including superior operating lifetimes, ultrafast charging–discharging rates, and high-power densities.[15–17] However, current electrodes with good electrochemical performance used in batteries and SCs are mainly based on relatively rigid and fragile electrodes and are unsuitable for flexible device fabrication because they show poor sustainability under complex stress environments. Meanwhile, the electrochemically inactive binder also could cause a loss of capacity and other safety problems.[18–20] Thus, binder-free electrodes for flexible energy storage devices emerged.

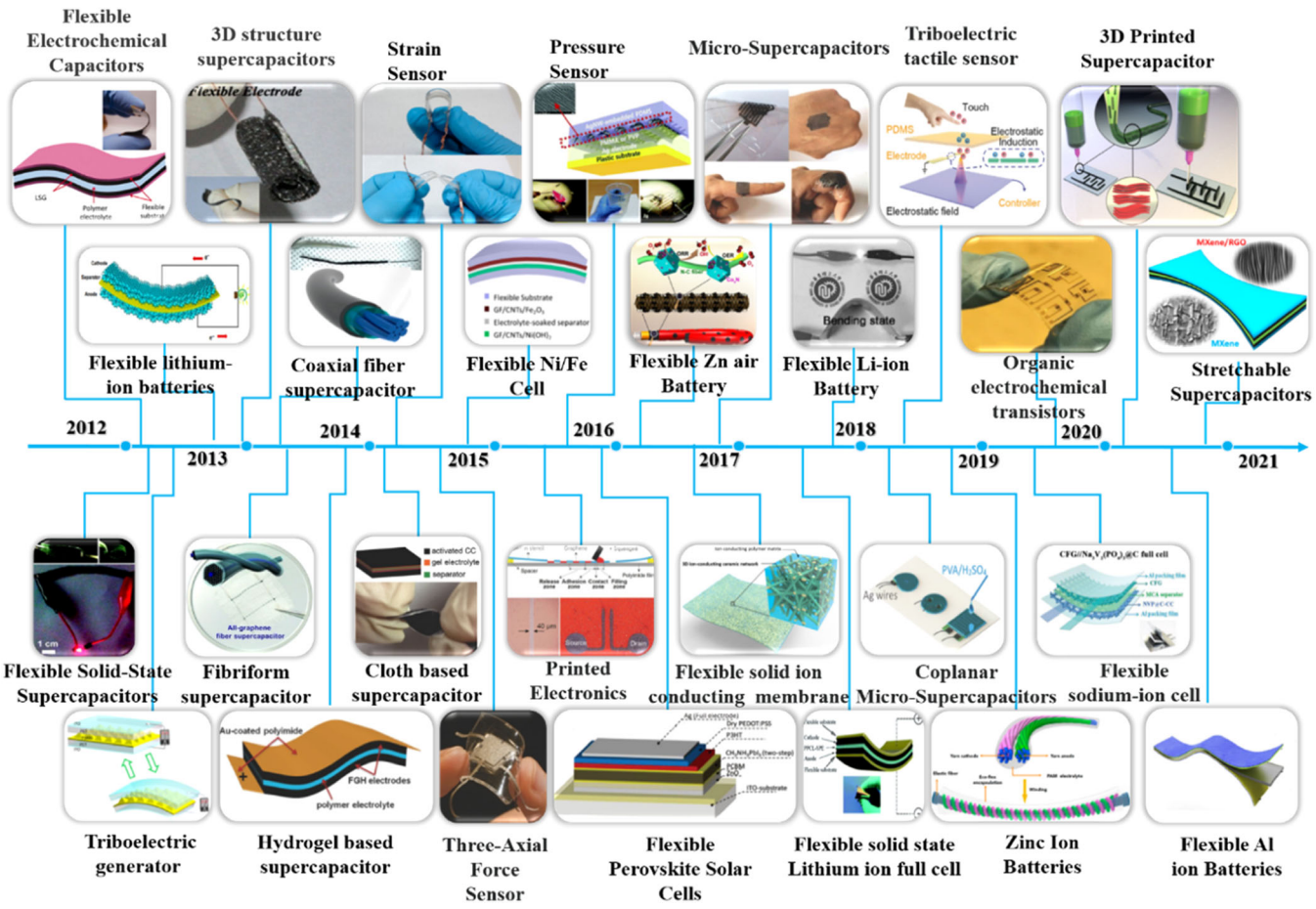

FIGURE 1 The evolution of flexible energy storage devices in previous reports.[21–47] Images reproduced with permission.

Based on recent developments, there are two strategies for fabricating flexible electrodes or components: first, synthesizing flexible freestanding films of active materials; second, depositing rigid active materials on flexible conductive or nonconducting substrates, a strong interaction between the active material and the substrate is generally required to maintain the structural integrity during deformation. Scientists endow flexible and stretchable materials with favorable electrochemical performance or rigid high-performance materials with a flexible nature through engineering. A schematic sketch of flexible batteries, SCs, and sensors with different designs and structures along with the types of electrodes used in their fabrication is given in Figure 2. This review concentrated on the recent progress on flexible energy-storage devices, including flexible batteries, SCs and sensors. In the first part, we review the latest fiber, planar and three-dimensional (3D)-based flexible devices with different solid-state electrolytes, and novel structures, along with their technological innovations and challenges. In the following section, a specific overview of the recent achievements about flexible electrolyte based on polymer, ceramic, and polymer/ceramic electrolyte are given, combined with a discussion of the problem and opportunities for the fabrication of the state-of-the-art flexible electrolyte. In the end, prospects and outlook on the future of flexible batteries are presented and discussed.

2 | FIBER-BASED WEARABLE ELECTRODES

Typically, the fiber usually has a large aspect ratio with a thickness or diameter in the scale of micron meters. These fibers can be further converted into various shapes (e.g., yarns, fabrics, and spacer fabrics) through well-established and cost-effective textile production processes. Meanwhile, advanced nanoscience and nanotechnology has made it feasible to build electronic modules under fiber technology and accelerate the miniaturization trend of electronic devices. Modern wearable electronics with the nature of fiber assemblies are endowed with the advantage of textile

FIGURE 2 Flexible energy storage devices and the types of electrodes used in their fabrication.

technologies, electrical engineering and electronics, and superior capacity. The hierarchical nature of these fibrous structures (fiber–yarn–fabric, etc.) makes them particularly suitable for the fabrication of wearable electronics. Carbon-based material, conductive polymer (PPy, PANI, PEDOT, etc.) and other one-dimensional (1D)-structured metallic wires, cotton thread, and yarn produced by spinning are the widely used substrates for fiber-type energy storage devices. This section reviews the current state of fiber-based energy storage devices with respect to conductive materials, fabrication techniques, and electronic components.

2.1 | Carbon nanotube (CNT)-based flexible electrodes

To meet the gradually increasing demands of portable electronics, it is significant to develop lightweight, flexible, and conformable electrodes for flexible electronics. For the realization of fiber-based wearable electronics, the most important consideration is the development of sustainable flexible systems which support high carrier mobility and good overall electrical performance, together with mechanical and environmental stability. Textile technologies offer tremendous opportunities to make sensors and other devices, built-in or embedded into the fabric-based network. So far, many composites such as reduced graphene oxide/nylon yarn,[48] Ag-silicone fibers,[49] fibers containing liquid metal alloy,[50] a conductive composite mat of silver nanoparticles and rubber fibers, and twisted graphene yarns[51] are designed for functional textiles and flexible and wearable battery devices. Among them, carbon-based materials are popular substrates for flexible electrode as they can act as both current collector and active materials.[52] For their favorable weavability, flexibility, and conductivity, CNT fibers as a typical 1D conductive material has been widely used in the fabrication of flexible electrode, which can be woven to form wearable cloths.[40,53] In Figure 3A, the $Li_4Ti_5O_{12}$ (LTO) and Li_2MnO_4 (LMO) particles were incorporated into two multiwalled carbon nanotube (MWCNT) threads by a soaking method, paired as anode and cathode to create a lithium-ion battery with a reversible capacity of 2.2 mAh m^{-1}. The elastic wire-shaped lithium-ion battery (Figure 3B) was assembled by winding above electrodes around an elastic substrate with a spring structure. As shown in the Figure 3C–D, the wire shpaed battery can be woven into the flexible textile. And the illumination intensity of the LED had no obvious change when the textile under geometric deformation.[54] Additionally, other functional guests (TiO_2, Si_3N_4, MnO_2, and Si nanowires) had been incorporated into the wires to improve the specific capacity of the devices.[55–59] The composite electrodes are expected to combine their individual advantage of high specific capacity, flexibility, and excellent conductivity. Peng et al. reported that a nanoscale Si layer was coated on the surface of the CNT sheets by atomic layer deposition (ALD). The core-shell-structured CNT@Si composites are endowed with the high specific capacitance of silicon and the good electrical conductivity of CNT (Figure 3E). The flexible composite fiber was obtained by a twisting treatment, which could bend for over a hundred cycles without an obvious decrease in the structure integrity. The specific capacity of it was maintained at 1460 mAh g^{-1} (96% of the initial specific capacity) after 100 times bending (Figure 3F–G). The good electrochemical performance can be attributed to the core-sheath structure, which could effectively counterbalance the volume change of Si. The aligned CNT enhances the charge transport between the CNT and Si.[55]

2.2 | Graphene-based flexible electrodes

Besides, graphene fiber with high strength and electrical conductivity represents another ideal type of fiber electrode.[60,61] It possesses the mechanical flexibility of common textile fibers and is modified easily in comparison with the conventional carbon fibers.[62,63] In 2012, Qu et al. fabricated the neat graphene fiber by a facile one-step dimensional-confined hydrothermal strategy. It has a tensile strength of 180 MPa and can be shaped to random geometry. The pliability of this fiber facilitates the weaving into various macroscopic objects.[64] Therefore, it has a great potential to be applied in stimulus-responsive and electronic textiles (Figures 4A–D). Along with the booming research on flexible batteries, motors, actuators, and dye-sensitized photovoltaic wires, SCs also have been designed based on the graphene fiber to expand their application.[42,65–67] Gao et al. prepared continuous graphene-Ag fiber with high electrical conductivity (9.3×10^4 S m^{-1}) and current capacity (7.1×10^3 A cm^{-2}), rendering the composite fibers good stretchable conductors to be applied in soft circuits.[68] Compared with batteries, SCs have a superior charge/discharge rate, ultrahigh power delivery, excellent cycle life and efficiency, a wide range of operating temperatures, and improved safety. Because it is easily incorporated into textiles, the fiber-shaped supercapacitor attracted widespread interest.[69–71] Peng's group also reported much work about fiber-shaped devices based on graphene.[54,55,57,59] With the graphene fiber as the core, nanorod-like polyaniline was deposited

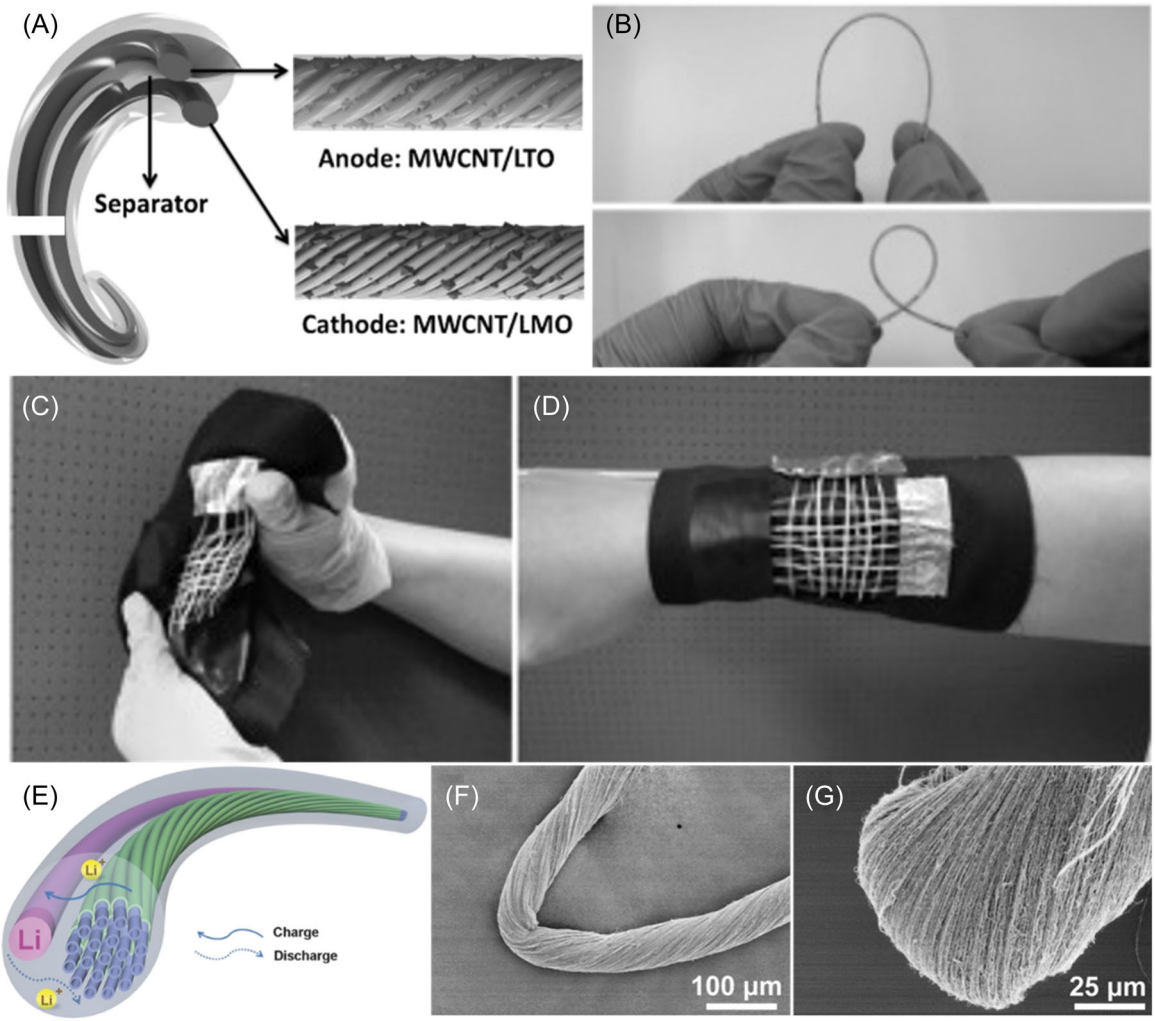

FIGURE 3 (A) The aligned multiwalled carbon nanotube (MWCNT)/LTO and MWCNT/LMO composite yarns are paired as the anode and cathode, respectively. (B) Photographs of a wire-shaped battery being deformed into different shapes. (C, D) Wire-shaped batteries woven into flexible textiles. Reproduced with permission.[54] Copyright 2014, Wiley. (E) Illustration of a half lithium-ion battery based on the aligned MWCNT/Si composite fiber. (F, G) Scanning electron microscope images of a bent aligned MWCNT/Si composite fiber. Reproduced with permission.[55] Copyright 2014, Wiley.

by an *in* situ chemical polymerization strategy (Figure 4E). The fabricated core-sheath fibers were twisted into all solid-state yarn-shaped SC with H_2SO_4/poly(vinyl alcohol) (PVA) gel electrolyte. The performance of this fiber-type device under bending has no change (Figure 4F). Moreover, three red LEDs were lighted by four SCs in series.[72] Wang et al. prepared a stretchable and self-healable supercapacitor by wrapping two parallel reduced graphene oxide fiber springs with a self-healing polymer shell (Figure 4G,H). At the power density of 7.32 mW cm^{-3}, a high energy of 0.94 mWh cm^{-3} was obtained. The capacitance retention is 82.4% after a large stretch (100%), while it is 54.2% after the third healing. It provides an essential strategy in next-generation multifunctional electronic device.[73]

2.3 | Flexible electronics based on other fiber-shaped substrates

Apart from the graphene and CNT, the conductive substrate like nickel fiber was also used to fabricate fiber-shaped devices. As depicted in Figure 5A, MWCNTs and vanadium oxide were used as the coating layer of the current collector of Au wire to enhance the overall supercapacitor performance via pseudocapacitance. Each electrode was dipped into the PC–ACN–$LiClO_4$–PMMA electrolyte.[74] Then, two electrodes were twisted to form a wire-shaped supercapacitor (WSS). It delivered an area capacitance of 5.23 mF cm^{-2} at 0.2 mA cm^{-2}; the capacitance retention under shape deformation varied from 97% to 104%, reasonably constant and equivalent to the original

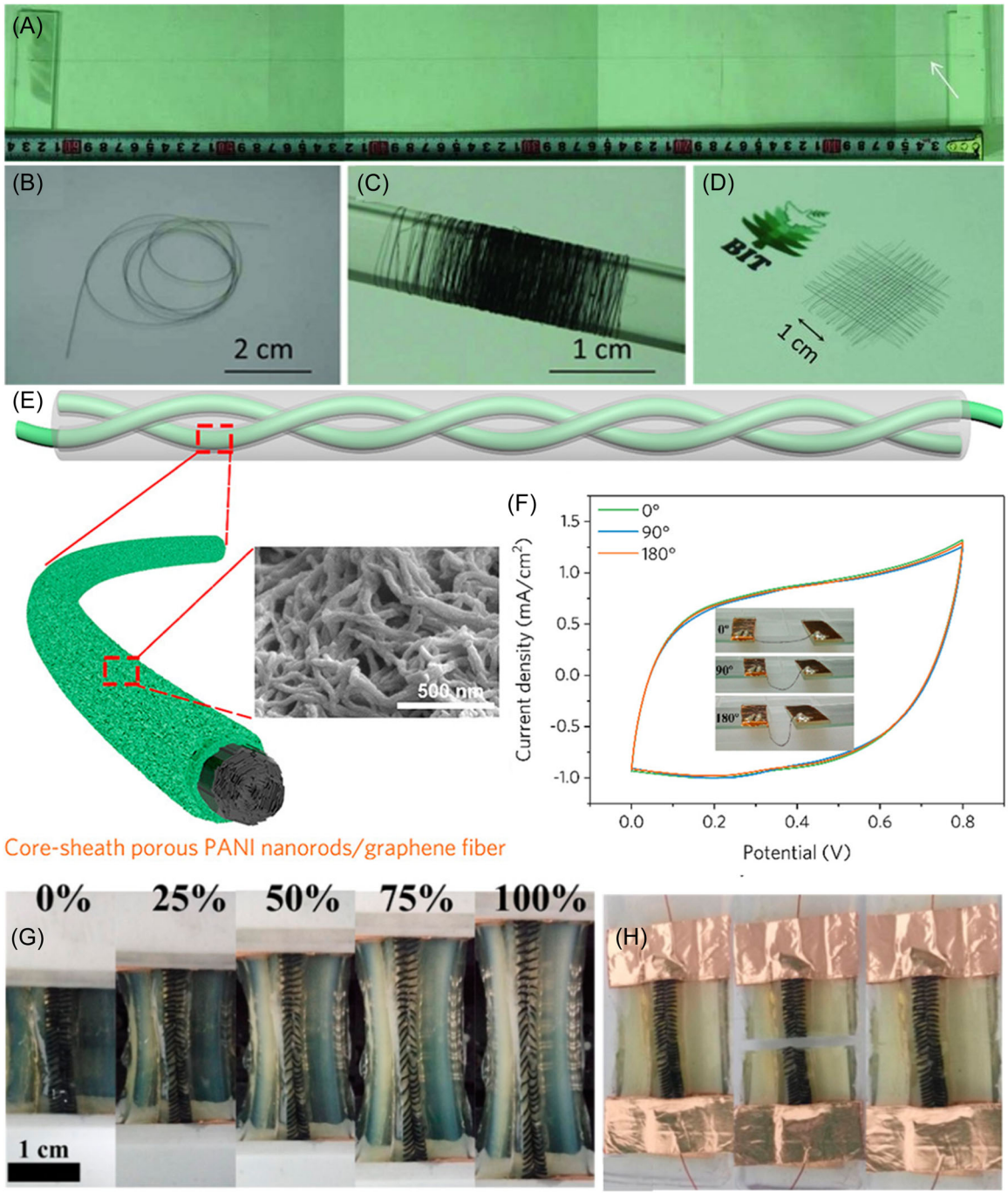

FIGURE 4 Morphology and flexibility of graphene fiber. Photograph of a single dry graphene fiber (A) with a diameter of ~33 μm and a length of 63 cm. (B) A wet graphene fiber coiled individually in water. (C) A dry graphene fiber coiled in bundle around the glass rod. (D) The hand-knitted textile of graphene fibers. Reproduced with permission.[64] Copyright 2014, Wiley. (E) Schematic diagram of the yarn-shaped supercapacitors. (F) CV curves of all-solid-state GF@PANI FSSC bended with 0°, 90°, and 180°. Reproduced with permission.[72] Copyright 2019, ACS. (G) Photographs of the supercapacitor before and after stretching to 100%. (H) Photographs of the supercapacitor before and after self-healing. Reproduced with permission.[73] Copyright 2017, ACS. CV, cyclic voltammetry.

capacitance. The nickel fiber with $Ni(OH)_2$ nanowire and the ordered mesoporous carbon fiber were twisted together with the KOH-PVA as the gel electrolyte, and a flexible micro-supercapacitor was obtained after further vaporizing water from the gel electrolyte. It presented 35.67 mF cm^{-2}, and the charge/discharge performance of the fiber-shaped supercapacitor is almost independent of the bending states.[75] Wang et al. demonstrated that polyester yarns coated with Ni were utilized as current collectors for electrodes in

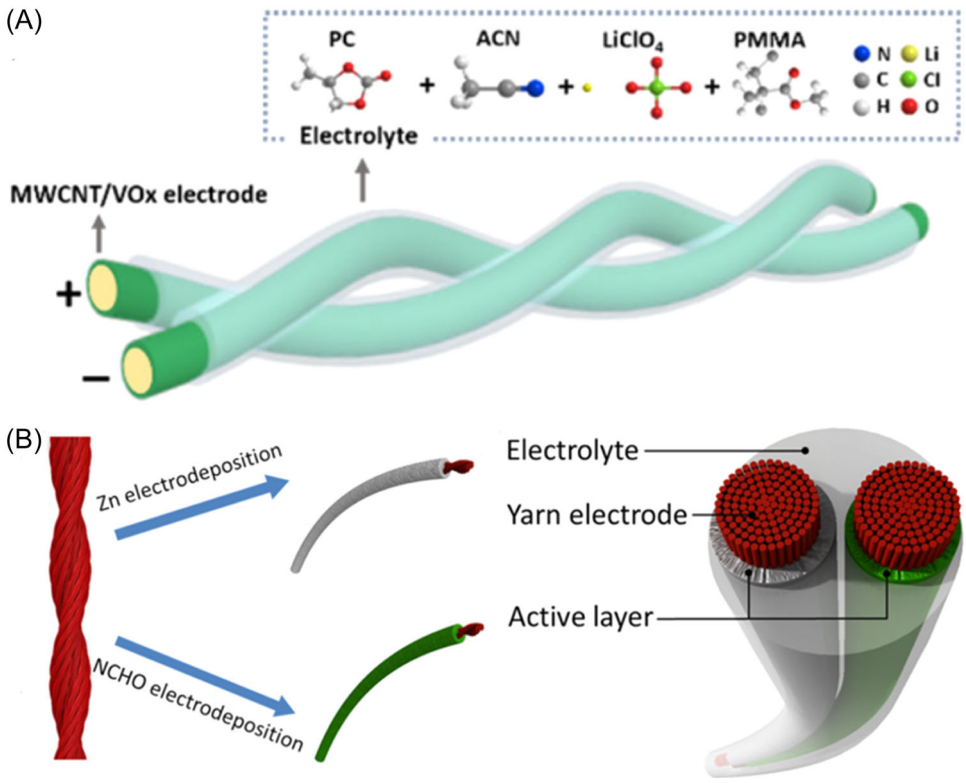

FIGURE 5 (A) The wire-shaped supercapacitor with a 100 μm thick Au wire, coated with multiwalled carbon nanotubes (MWCNTs) and vanadium oxide (VOx) and an organic electrolyte. Reproduced with permission.[74] Copyright 2018, ACS. (B) Schematics of a free-standing solid-state yarn NiCo//Zn battery. Reproduced with permission.[77] Copyright 2017, ACS.

all-solid-state yarn SCs. The rGO layer was coated on the electrode as active materials. Two rGO-Ni-yarns in parallel and PVA/H_3PO_4 gel as solid electrolyte and separator were assembled into a symmetric yarn supercapacitor.[76] After bending 1000 cycles by a motor, the capacitance of this yarn supercapacitor shows no significant difference. As for wearable energy-storing textiles, it can withstand harsh deformation. Five yarn SCs were connected in series and were woven into a piece of fabric together with common cotton yarns. This soft energy-storing fabric can light a red light-emitting diode (LED). In addition, flexible zinc-ion batteries and other alkaline batteries have been fabricated. Huang et al. reported that bimetallic hydroxides could deliver higher capacity because of the synergistic effects between transition metal ions (Figure 5B). Zinc and nickel cobalt hydroxide nanosheets were electrodeposited on the highly conductive yarn. The solid-state yarn battery delivered a maximum volumetric density of 8 mWh cm^{-3}. The device has shown good weavability and flexibility.[77] Zhi et al. also reported a flexible, high-performance yarn zinc-ion battery using double-helix yarn electrodes and a cross-linked polyacrylamide (PAM) electrolyte.[27]

In addition to the twisted or spring structure, a novel concept for electronic devices architecture—tube-type devices show superior mechanical flexibility. A heat-shrinkable tube is used to encapsulate the device and provides sufficient pressure for holding all components closely.[78] For instance, the tube-type lithium-ion battery is composited by a hollow helix anode (Ni/Sn -coated Cu wires), a modified polyethylene terephthalate (PET) nonwoven separator, and a rigid cathode (Figure 6A,B). The fiber shape and omni-directional flexibility of the cable battery make it can be placed anywhere and in any shape. Moreover, the cable battery could be worn on the weaved into different types to meet the requirements of our daily life, which will facilitate the realization of practical wearable electronics. The cable battery shows good charge/discharge behaviors and stable capacity retention, similar to its designed cell capacity (per unit length of the cable battery) of 1 mA h cm^{-1} under a voltage range of 2.5–4.2 V.[79] With further optimization of the battery components, the cable-type battery will undoubtedly have a great impact on the fields of portable, wearable, and flexible electronics. In the Figure 6C,D, a tube-type flexible SIBs are fabricated based on cotton textile coated by Ni, Prussian blue and graphene. For its practical use, a commercial light emitting diode was lighted, even though the battery is intentionally bent and spiral (Figure 6E,F).[80] Meanwhile, the yolk-shell NiS_2 @ porous carbon fiber electrode was fabricated by vapor

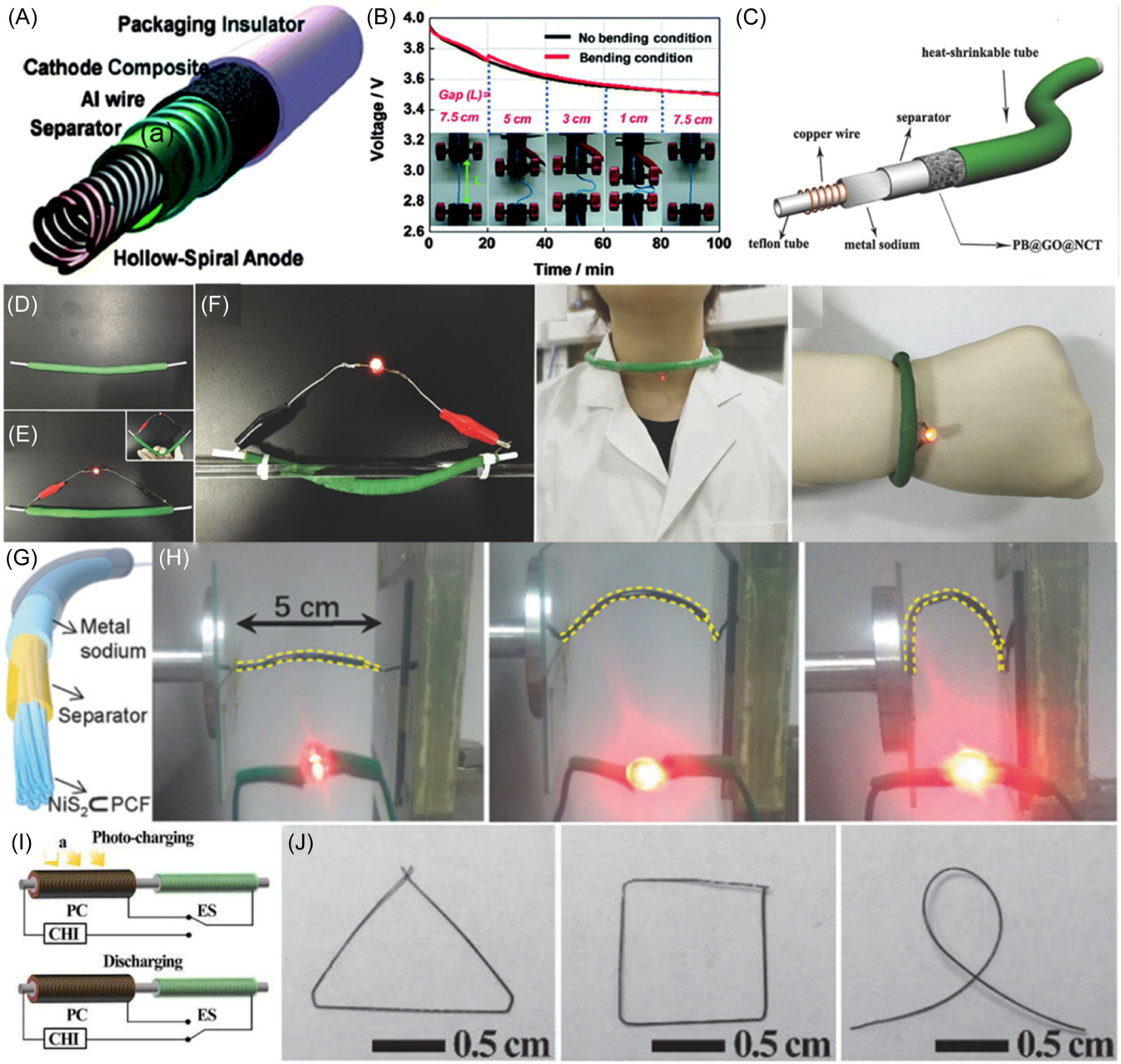

FIGURE 6 (A) Schematic illustration of the cable battery with hollow-helix anode having multiple-helix structure. (B) Discharge characteristics with variations in bending strain every 20 min. Reproduced with permission.[79] Copyright 2012, Wiley. (C) Schematic illustration for the structure of the tube-type flexible SIBs. (D) Digital photograph of the fabricated tube-type flexible sodium-ion battery (SIBs). (E, F) Demonstration of an light-emitting diode (LED) lighting by tube-type flexible SIBs under different conditions. Reproduced with permission.[80] Copyright 2017, Wiley. (G) Schematic illustration for the construction structure of the flexible fiber-shaped sodium battery and (H) photos of LEDs lightened by as-assembled fiber-shaped sodium battery under different bending states. Reproduced with permission.[81] Copyright 2018, Wiley. (I) Schematic diagram shows the circuit connection state in the process of charging and discharging. (J) Photograph of "energy fibers" being bent into various shapes. Reproduced with permission.[83] Copyright 2014, Wiley.

deposition. The tube-type concept was also used to design the flexible fiber-shaped sodium-ion battery (Figure 6G,H). It showed stable performance under different bending conditions. Even at high bending angles of 120° and 150°, only 9% and 11% of reversible capacity reduction occurred.[81] The graphene/CNT composite fiber also had been applied as electrodes to produce wire-shaped dye-sensitized solar cells with photoelectric conversion efficiencies up to 8.50% and SCs with specific capacitances up to ~31.50 F g^{-1} (4.97 mF cm^{-2} or 27.1 μF cm^{-1}), much higher than the bare CNT fibers under the same condition.[82] Based on the concept of self-powering, the application of energy-harvesting

technologies from the ambient environment for sustainable operation may be the most promising alternative to meet the increasing energy requirement. The explored fiber-shaped integrated energy devices attracted much more attention. A novel, all-solid-state, flexible "energy fiber" that integrated the functions of photovoltaic conversion and energy storage has been made based on titania nanotube-modified Ti wire and aligned MWCNT sheet as two electrodes. the "energy fiber" could be bent into various forms depending on the application requirement. And the entire photoelectric conversion and storage efficiency during bending was slightly decreased by less than 10% after bending for 1000 cycles without sealing.[83] In Figure 6I,J, an SC-triboelectric nanogenerator power system was designed, which can harvest mechanical energy from human motion. In this system, the nanogenerator charges supercapacitor by the contact-electrification and electrostatic-induction process, demonstrating that this self-charging power system is a very promising concept to meet the increasing demands of flexible power sources in wearable electronics.[84,85]

3 | THE PAPER-LIKE STRUCTURED ELECTRODES

Different from the conventional electrodes prepared via the slurry-coating method, free-standing materials can be utilized directly as electrodes or substrates to support rigid active materials without binder, conductive additive, and even metal current collector.

3.1 | Flexible electrodes based on conductive substrate

Up to now, carbon-based materials such as CNTs, graphene, carbon fiber, and carbon cloth can be easily assembled into flexible membranes by vacuum filtration, self-assembly, dry-drawing, blade-coating, and ink printing. A versatile approach to achieving flexible electrodes is to filter solutions containing nanosized active materials with flexible substrates (CNT, graphene, cellulose, and PAN) and other two-dimensional layered material (transition metal dichalcogenides: e.g., MoS_2 and WS_2). The active materials offer substantial specific capacity, while the CNTs and graphene provide both electronic conductivity and mechanical support. Moreover, surface modifications of the conductive substrates are required to enable solution processing and enhance the electronic conductivity. Flexible electrodes composited by these materials showed impressive electrochemical performances. Researchers mostly focused on finding new electrode materials and unique structure with a highly conductive pathway for electrons, a short ion diffusion length, and a fast transport channel for ion delivery. Graphene-based films have been obtained by spin-coating, layer-by-layer, and vacuum filtration. For example, Liu et al. reported that a folded structured graphene paper is obtained by freeze-drying and thermal reducing of a GO aqueous dispersion. This paper-like graphene is free-standing and flexible. The folded structure of the graphene sheets with fewer layers could provide more lithium insertion active sites, such as edge-type sites and nanopores. As electrodes for LIB, it shows first discharge and charge capacity are 1091 and 864 $mA\,h\,g^{-1}$, corresponding to the initial Coulombic efficiency of 79.2%.[86] Moreover, a graphene-based flexible electrode was applied both to a cathode and anode by using a pulsed laser deposition technique. A reversible capacity of 21 $\mu Ah\,cm^{-2}$ was observed for nanostructured V_2O_5/graphene paper, which is significantly improved than that reported previously for thin film electrodes with amorphous V_2O_5.[87] Besides that, ultrathin and flexible graphene paper have also been used for supercapacitors. For instance, a porous graphene film was fabricated by a template method and filtration. PANI nanowire arrays were grown on the surface of the film. This composite film was assembled into a flexible supercapacitor by using Au-coated polyimide film as both the current collector and encapsulating material. Based on the cyclic voltammetry (CV) curves under different bending statuses, the geometry deformation has no effect on the performance of the flexible devices.[88]

Similarly, free-standing MWNT thin films were prepared by a simple lamination process, electrospinning, weaving, or vacuum filtration, which was used as current collectors for both anode and cathode. In 2007, flexible batteries and SCs based on cellulose paper embedded with CNT and room-temperature ionic liquids (ILs) electrolyte were designed. Unmodified plant cellulose dissolved in RTIL ([bmIm][Cl]) is infiltrated into the MWNT to form a uniform film of cellulose and [bmIm][Cl], embedding the MWNT. After solidification on dry ice and removing excess RTIL and ethanol, the resulting nanocomposite paper forms the basic building unit in those flexible devices.[89] Hu et al. also demonstrated that the free-standing, lightweight CNT films were used as the collectors, and $Li_4Ti_5O_{12}$ and $LiCoO_2$ slurries were coated on CNT films by a simple lamination process. The whole device was sealed with 10 μm PDMS. No failure was observed for the paper battery after manually bending the device down to 6 mm 50 times.[90] Xiao et al. reported a free-standing mesoporous vanadium nitride (VN)/CNT hybrid electrode prepared by vacuum filtration of a solution mixture of VN nanobelts and CNTs. Both VN and CNT have excellent electrical conductivity that ensures its

application as electrode without current collectors. CNT and graphene suffer from a large irreversible capacity, low initial Coulombic efficiency, and fast capacity fading, which are mainly due to the re-stacking structure and side reactions between carbon materials and electrolytes arising from the functional groups and defects of the carbon materials.[91]

To improve the capacity and cycling stability, heteroatoms (N, B, S, and P) doping, nanostructured Si, Sn, and metal oxides (Co_3O_4, SnO_2, TiO_2, Mn_3O_4, Fe_2O_3, etc.), and transition metal dichalcogenides (TMDCs, e.g., MoS_2 and WS_2) have been used to modify the free-standing substrates.[92–95] Heteroatom doping with nitrogen and boron could induce a large number of defects, leading to an increase in the reversible capacity,[68,96,97] while the nanostructure could accommodate the strain of lithium insertion/extraction, increase the contact area between electrode and electrolyte, and short the path lengths for electronic and ions transport.[98] As shown in Figure 7A–D, hierarchical $ZnCo_2O_4$ nanowire arrays/carbon cloth shows a high capacity of 1300 mA h g^{-1} and maintains 96% of the initial capacity after 40 cycles. The 3D configuration of the composite greatly increases the electrolyte/$ZnCo_2O_4$ contact area. The loose textile accommodates the strain induced by the volume change during electrochemical reactions.[99] Meanwhile, various carbon additives have also been mixed with the metal oxide particles to improve their conductivity. For instance, vanadium oxide (V_2O_5) nanowires were synthesized by hydrothermal reaction based on the network of ultra-long CNTs. The composite electrodes with 25 wt.% CNTs show a strength of 4.7 MPa, which is significantly higher than that of CNT and V_2O_5 nanowire electrodes. It also exhibits 318 mAh g^{-1} at the current

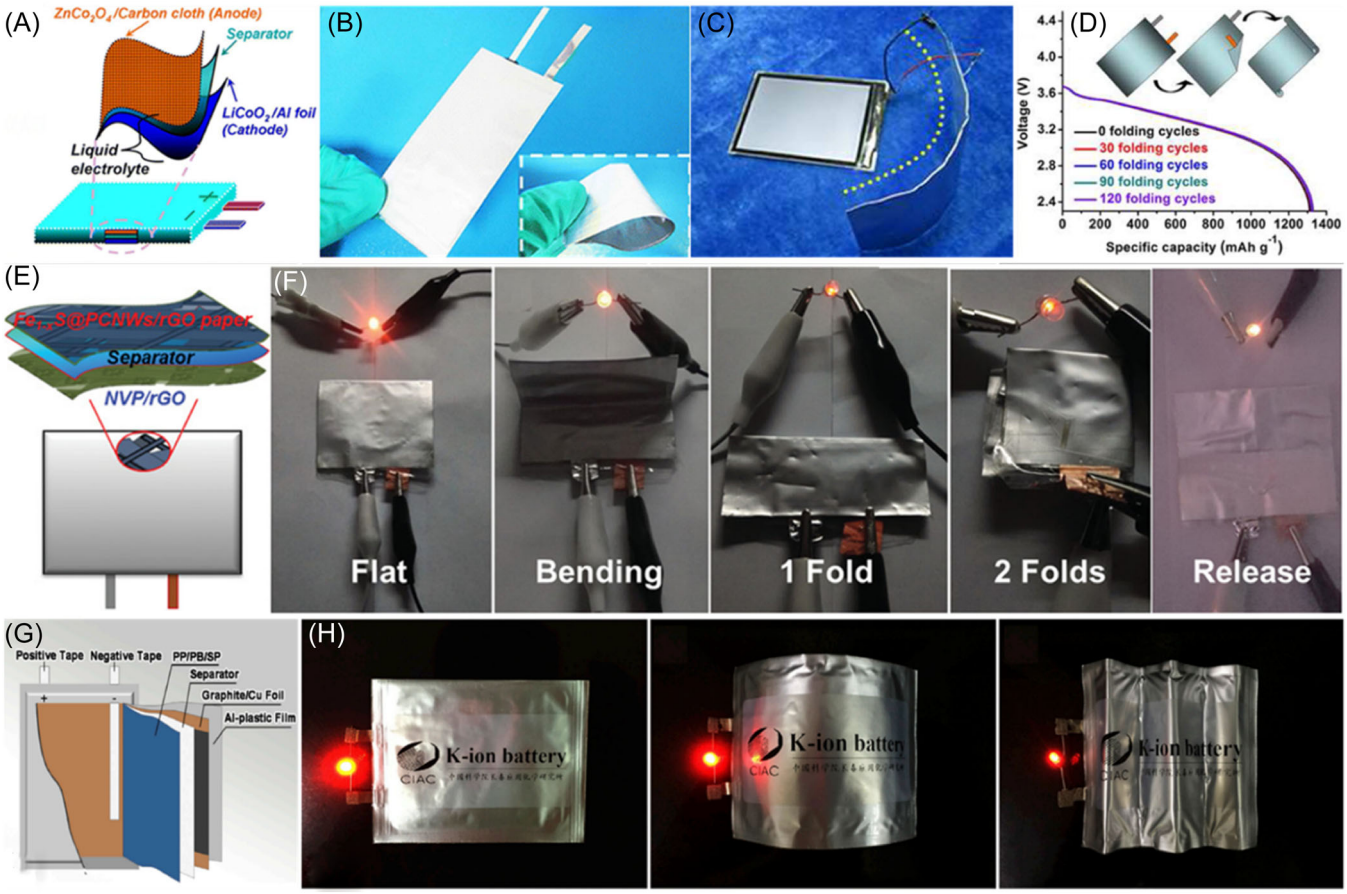

FIGURE 7 (A) Schematic illustration for the fabrication of the hierarchical three-dimensional $ZnCo_2O_4$ nanowire arrays/carbon cloth/liquid electrolyte/$LiCoO_2$ flexible lithium-ion battery. (B) Photograph of the fabricated flexible Li-ion battery. (C) The digital photo of tuning on a mobile phone screen by a foldable battery. (D) The voltage versus specific capacity profiles of full flexible battery before and after 30, 60, 90, and 120 cycles of bending.[99] Reproduced with permission.[99] Copyright 2012, ACS. (E) Schematic illustration for fabrication of the flexible sodium ion battery (SIB) and its structure. (F) Digital photos of the flexible SIB lightening an light-emitting diode (LED) under various states. Reproduced with permission.[102] Copyright 2019, Wiley. (G) Photographs of the fabricated, flexible potassium-ion batteries (KIBs). (H) Demonstration of an LED light by flexible KIBs under flat, bending, and folding states. Reproduced with permission.[103] Copyright 2018, ELSEVIER.

density of 70 mA g^{-1}.[100] David et al. demonstrated the synthesis of a composite-layered paper consisting of acid-exfoliated MoS_2 nanoflakes in an rGO matrix with mechanical strength 2–3 MPa and high failure strain (approximately 2%). The electrode stabilized to a charge capacity of 240 mAh g^{-1} at a current density of 25 mA g^{-1} (with respect to the total weight of the electrode) after the initial five cycles.[101] Carbon cloth, commonly termed as CC, a highly conductive textile with superior mechanical flexibility and strength than graphene, CNTs, and cellulose paper, holds a great commitment to serving as a flexible substrate in the fabrication of flexible energy storage devices. To date, numerous flexible energy storage devices have rapidly emerged, including flexible lithium-ion batteries (LIBs), sodium-ion batteries (SIBs), lithium-O_2 batteries. In Figure 7E,F, a $Fe_{1-x}S$@PCNWs/rGO hybrid paper was also fabricated by vacuum filtration, which displays superior flexibility and mechanical properties. A flexible packaged full cell is fabricated. As demonstrated, it works well under a continuous bending process.[102] Therefore, the flexible potassium-ion batteries (KIBs) come into being. Highly crystalline Prussian blue (PB) nanocubes were synthesized onto Xuan paper by cyanotype, which is a novel photographic printing strategy. The photographic printing flexible PB cathode and graphite/Cu anode were assembled in a flexible device, which is sealed by Al-plastic film. For practical applications, an LED could be lighted even though the device is intentionally bent and folded (Figure 7G,H). Its discharge capacity remains almost unchanged under different geometric deformations (bent and folded).[103,104] Graphene sheets are also used to incorporate high storage capacity Si, employing as a stable and self-supporting composite electrode with enhanced accessible interior and high-rate capacity.[105–107] By magnesiothermic reduction and layer-by-layer assembly process, an inter-overlapped Si hollow nanosheet and rGO flexible electrode was obtained for flexible LIB (Figure 8A,B). The Si/rGO films deliver a high specific capacity of 904 mAh g^{-1} at 200 mA g^{-1} and possess an excellent stability (650 mAh g^{-1} after 150 cycles). From Figure 8C, the capacitance is not affected by the deformation of the flexible LIB.[107]

Compared with secondary rechargeable batteries with volatile and flammable organic electrolytes, aqueous rechargeable batteries are more promising considering the cost and safety as well as the ionic conductivity of electrolyte.[111] The successful realization of the flexibility of such kinds of batteries provides an effective strategy to enrich the family of flexible energy storage systems. Flexible devices such as nickel–metal (i.e., cadmium, iron, zinc, or Bismuth),[38,112,113] Zn–MnO_2 battery,[114–118] and alkali-ion battery[119,120] exhibit high ionic conductivity, environmental issues, good safety, and low cost. Much more efforts have been devoted to developing novelty cheap electrodes with unique nanostructures to meet the flexibility and energy storage requirement.[121–123] Rechargeable Ni–Fe batteries were assembled by direct growth of $Ni(OH)_2$ nanosheets and mesoporous Fe_2O_3 nanorods on the GF/CNTs hybrid films. Two flexible poly(ethylene terephthalate) (PET) sheets were used as flexible substrates. The Ni/Fe cell exhibited an energy density of 100.7 Wh kg^{-1} at 287 W kg^{-1}. Moreover, the cell also shows good cycling stability with a capacity retention of 89.1% after 1000 cycles. There were little changes in the charge/discharge curves at different bending angles (up to 60°).[38] Compared with other aqueous batteries, Ni–Zn battery has a high output voltage. But the cycle stability is usually very poor. The nanostructure can be a cushion of the shape change during charge and discharge and effectively suppress the Zn dendrite growth. It also facilitated electrolyte penetration and fast ion/mass transport. Therefore, ZnO and NiO nanoparticles have been deposited on the 3D network carbon cloth-carbon nanofiber substrate (Figure 8D). The full-cell quasi-solid-state device showed good suitability to shape deformation and 91.45% capacity retention after 1000 cycles.[108] Li et al. designed a solar-charged planar flexible quasi-solid-state Ag-Zn battery (Figure 8E,F). Carbon cloth coated with Ag nanowires and Zn nanoflakes was used as flexible cathode and anode. Eventually, a flexible device was obtained with KOH-PVA gel electrolyte in a classic sandwich structure. It delivers a capacity of 1.245 mAh cm^{-2}, which is not obviously different at various angles from 0 to 135°.[109]

Besides the above batteries, an energy storage system based on a battery electrode and a supercapacitor electrode called battery-supercapacitor hybrid (BSH) offers a promising way to construct a device with merits of both secondary batteries and SCs. In 2001, the hybrid energy storage cell was first reported by Amatucci. An activated carbon cathode and nanostructured $Li_4Ti_5O_{12}$ anode were assembled into the cell.[124] Li-ion BSHs systems with organic electrolytes could work under a wider potential window, and hence much higher energy density is obtained. For example, materials used as Li-insertion hosts are $Li_4Ti_5O_{12}$ (LTO),[125] Nb_2O_5,[126] V_2O_5,[127] $LiMn_2O_4$,[128] and $Li_3V_2(PO_4)_3$.[129] Aqueous Li-ion BSHs is an attractive hybrid device due to the high safety (nonvolatile, nonflammable, and nontoxicity) and high ionic conductivity of aqueous electrolytes as well as the facile device assembly process. They usually use neutral aqueous lithium-salt solutions (Li_2SO_4, $LiNO_3$, and LiCl) as electrolytes. A high-performance solid-state CNTs $(CNTs)_{(+)}//Fe_3O_4–C_{(-)}$ alkaline battery-supercapacitor hybrid device was constructed, which delivered a volumetric energy density of 1.56 mWh cm^{-3}.

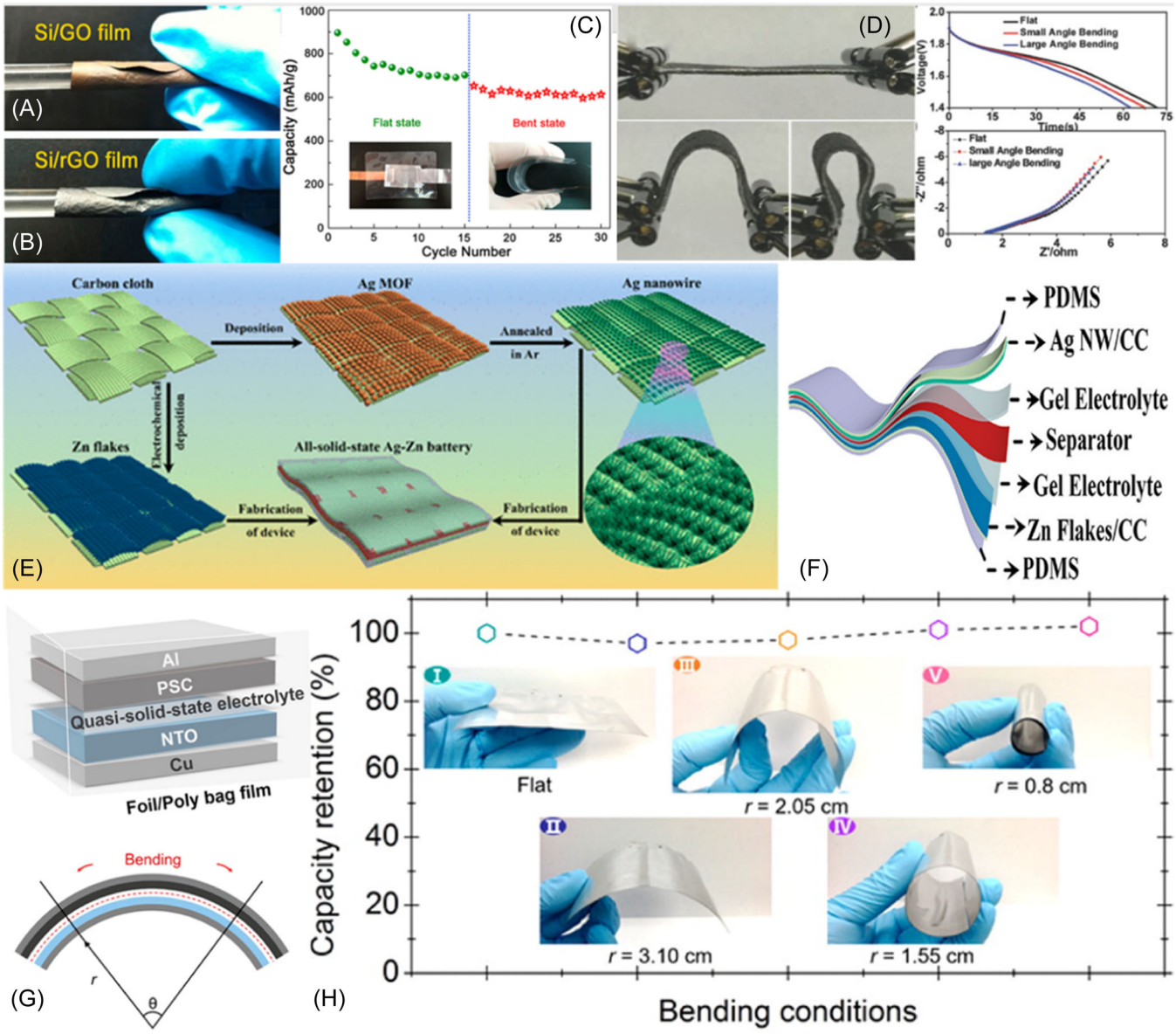

FIGURE 8 (A, B) Photos of Si/rGO flexible film in different states; (C) Electrochemical performance of the flexible full lithium-ion batteries for 15 cycles at 50 mA g^{-1} in both flat and bent state. (D) Discharge curves and EIS results of flexible quasi-solid-state Ni–Zn battery with different bending conditions. Reproduced with permission.[108] Copyright 2016, Wiley. (E) Schematic illustration of the synthesis of the flexible quasi-solid-state Ag-Zn battery; (F) Schematic diagram of the fabricated flexible quasi-solid-state Ag–Zn battery. Reproduced with permission.[109] Copyright 2018, ACS. (G) Schematic illustration of the structure of the quasi-solid-state sodium ion capacitor. (H) Stability of capacitive performance of the quasi-solid-state sodium ion capacitor collected at different bending conditions (the inset shows the flexibility with different mandrel radius). Reproduced with permission.[110] Copyright 2016, ACS. EIS, electrochemical impendance spectroscopy.

This solid-state hybrid device also can withstand mechanical deformation and different environmental temperatures ranging from 20°C to 100°C.[130] Li et al. demonstrated that a quasi-solid-state Na-ion BSH was designed using the PVDF-HFP membrane as the matrix of gel electrolyte. The urchin-like $Na_2Ti_3O_7$ and activated carbon derived from peanut shells were used as anode and cathode (Figure 8G). A high-energy density of 111.2 W h kg^{-1} is achieved at a power density of 800 W kg^{-1}. In addition, the capacity could maintain 86% after 3000 cycles. There is no obvious loss of capacity under different bending (Figure 8H).[110,131–136]

3.2 | Flexible electrodes based on nonconductive substrate

As it turns out, graphene, CNT, and carbon cloth have good film-forming property. However, the mechanical performance of pure carbon materials is not

sufficient. Therefore, polydimethylsiloxane (PDMS), cellulose paper, PET, and polymethylmethacrylate (PMMA) with superior mechanical performance are introduced to support the active material. Many electronic materials can provide good bendability when prepared in thin-film form and placed on thin substrate sheets or near neutral mechanical planes in substrate laminates.[137–141] In Figure 9A–E, sandwich-structured flexible device has been fabricated by using cellulose paper as the flexible supporting layer. It shows superior mechanical property and can undergo severe bending.[141] A graphene-cellulose paper was designed that combined the conductivity and electroactivity of graphene and excellent mechanical property of cellulose paper. It presented a stress of 8.67 MPa and an elongation of 3%, which is much more superior than the pure graphene paper.[139] PPy, PANI, PEDOT, PSS, PMT, and other conductive polymers were usually used to enhance the conductivity of insulated and flexible substrate such as cellulose paper, PDMS, and PTFE membrane.[142–144] A low-temperature hydrothermal method was used to fabricate a piezoelectric nanogenerator. ZnS-NRs and conducting filler (PANI or MWCNTs) were dispersed in the PDMS matrix to form a composite film. The geometric deformation (rolling, twisting, folding, and

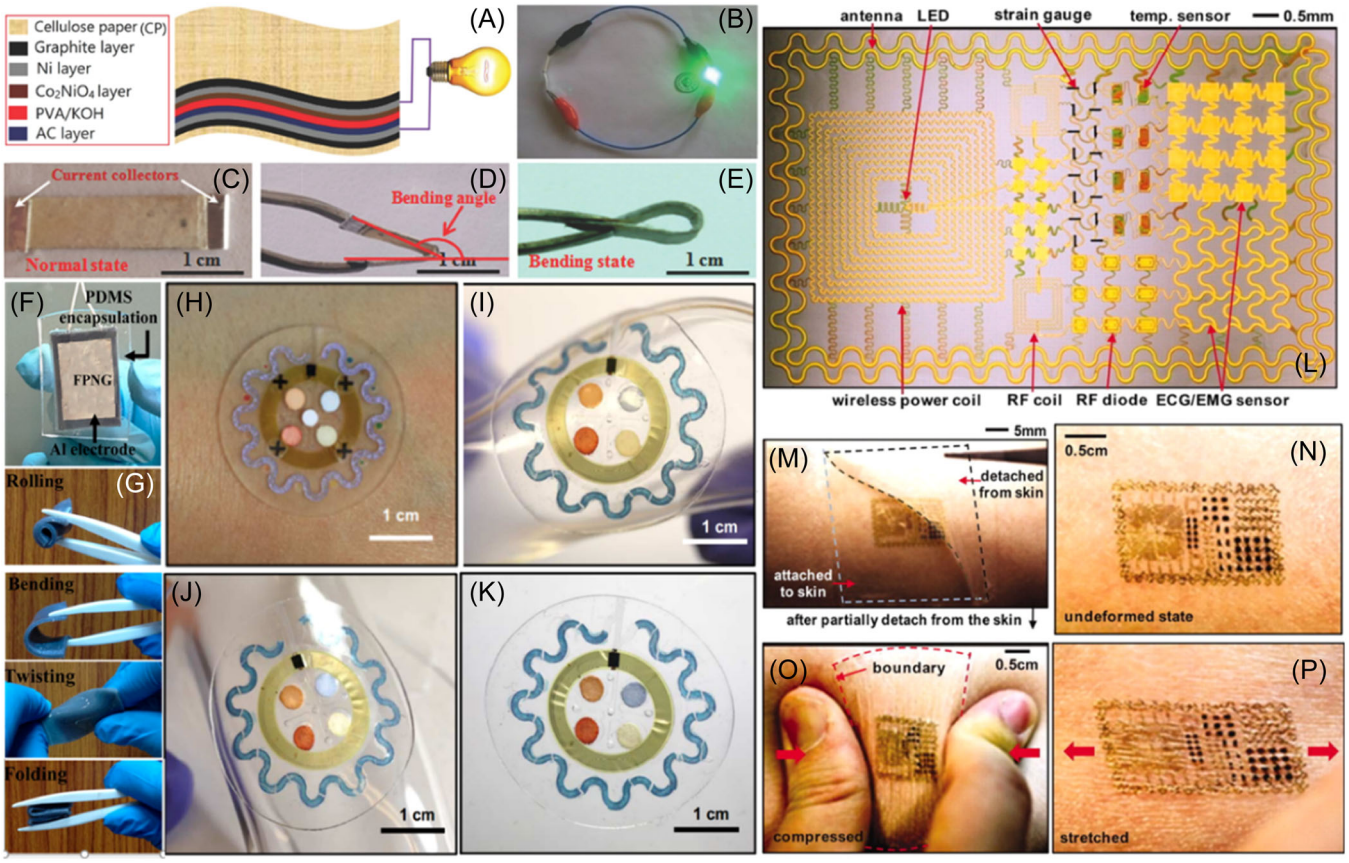

FIGURE 9 (A) Schematic illustration for the assembled graphite/Ni/Co_2NiO_4-CP//graphite/Ni/AC-CP ATFSCs; (B) A light-emitting diode (LED) powered by 2 ATFSCs in series; The flexible assembled ATFSCs: (C) normal state, (D, E) bending states. Reproduced with permission.[141] Copyright 2014, Wiley. (F) A digital photographic image of PDMS encapsulated PZP-FPNG with Al electrodes. (G) The flexibility of the PZP-FPNG is demonstrated by rolling, twisting, folding, and bending states. Reproduced with permission.[145] Copyright 2015, ACS. (H) Optical image of a fabricated device mounted on the forearm. (I–K) FEA results of stress distribution associated with the devices on phantom skin (PDMS) and respective optical images under various mechanical distortions: stretching at 30% strain, bending with 5 cm radius, and twisting. Reproduced with permission.[148] Copyright 2016, American Association for the Advancement of Science. (L) Image of a demonstration platform for multifunctional electronics with physical properties matched to the epidermis. Mounting this device on a sacrificial, water-soluble film of poly(vinyl alcohol) (PVA), placing the entire structure against the skin, with electronics facing down, and then dissolving the PVA leaves the device conformally attached to the skin through van der Waals forces alone, in a format that imposes negligible mass or mechanical loading effects on the skin. (M) EES partially peeled away from the skin. Multifunctional EES on skin: undeformed (N), compressed (O), and stretched (P). Reproduced with permission.[149] Copyright 2011, American Association for the Advancement of Science. EES, epidermal electronic system; FEA, finite element analysis.

bending) demonstrates the flexibility of the flexible piezoelectric nanogenerator (Figure 9F,G). Furthermore, this device is tested for wireless detection of pressure impact (~13.6 kPa) in terms of output voltage/response.[145] In a tetrahedral unit of ZnS-NRs, the relative displacement of the positive and negative charge centers under stress creates a dipole moment. And the total dipole moment results in a macroscopic piezoelectric potential. CNF/PDMS aerogel film was obtained by freeze-drying, sandwiched between two thin PDMS films and aluminum foils, to form flexible piezoelectric nanogenerators. Under periodic external mechanical stimulation, the output signal is stable and high.[146] Patterned PDMS is also used as a supporting layer of an array of GaAs for stretchable inorganic photovoltaic devices.[147] An ultrathin, light, and flexible organic photovoltaic device was constructed on PET substrates. It showed extreme mechanical resilience, which survived quasi-linear compression to below 70% of their original area.[3]

In Figure 9H–K, a microfluidic system was constructed on a flexible and patterned PDMS substrate with reagents for colorimetric analysis. This bioelectronic can maintain the structure under geometric deformation (stretching, bending, and twisting).[148] Although these systems show significant functions, they cannot make a real impact on our lives. It is difficult to build a long-period, strong electrical contact without irritating the electronic skin and achieve integrated systems with different electronic elements that do not cause discomfort during prolonged use. Indeed, skin can be regarded as a signal source: It can both generate and transmit biological signals that provide important health metrics of an individual. Research inspired by this multifunctional biological model has been developing large-area networks of sensors that can detect pressure, temperature, and other environmental stimuli. Organic and inorganic materials have been used to fabricate artificial electronic skins. A variety of sensors (e.g., mechanical[150,151] and temperature sensors[152,153]) integrated on plastic and/or elastomeric substrates can capture signals, simulating mechano- and thermo-receptor properties of skin tissues. Toward this end, multifunctional sensors (temperature, strain, and electrophysiological), microscale LEDs, circuit elements (such as transistors, diodes, and resistors), wireless power coils, and high-frequency inductors, capacitors, oscillators, and antennae, all integrated on the surface of a thin (~30 μm), gas-permeable elastomeric sheet based on a modified polyester (BASF) with low Young's modulus (~60 kPa). As shown in Figure 9L–P, the devices and interconnects exploit ultrathin layouts (<7 μm), neutral mechanical plane configurations, and optimized geometrical designs. The active elements use established electronic materials, such as silicon and gallium arsenide, in the form of filamentary serpentine nanoribbons, micromembranes and nanomembranes. The result is a high-performance system that offers reversible, elastic responses to large strain deformations with effective moduli (<150 kPa), bending stiffnesses (<1 nN m), and areal mass densities (<3.8 mg/cm^2) that are orders of magnitude smaller than those possible with conventional electronics or even with recently explored flexible/stretchable device technologies.[149]

4 | THE 3D STRUCTURED ELECTRODE

Currently, 3D electroactive nanostructured materials grown directly on conductive substrates as binder-free integrated electrodes for batteries is an emerging new concept, which can not only avoid the "dead surface" in conventional slurry-painted electrodes and allow for more efficient electron transport but also simplify electrode fabrication. Here, we just discuss the 3D materials that are stretchable and compressible on the micro and macro aspects. 3D porous frameworks possess multidimensional electron transport pathways, easy access to the electrolyte, and minimized transport distances between bulk electrode and electrolyte. Recently, significant research efforts have been focused on 3D interconnected networks (such as aerogels, hydrogels, and foams) as current collector or matrix and scaffolds via hydrothermal, layer-by-layer assembly, and chemical vapor deposition methods.

Chen and his coworkers first synthesized graphene foam (GF) by the CVD method (Figure 10A,B).[154] After combining with PDMS, the obtained free-standing GF is extremely light and flexible with high conductivity. And the resistance of the GF/PDMS composite became stable after several cycles of bending or stretching. This composite also showed shielding effectiveness of 30 dB in the 30 MHz–1.5 GHz frequency range and 20 dB in the X-band frequency range. More importantly, the specific EMI shielding effectiveness can reach 500 dB cm^3 g^{-1}. No obvious performance degradation is observed under the mechanical deformation.[155] Inspired by this work, the similar 3D structured materials showed the great potential application of nanogenerators, SCs, and other energy storage systems.[156–159] Typical 3D structured aerogels and hydrogel could be easily obtained by the reduction of a graphene oxide dispersion, in which flexible graphene sheets partially overlap in 3D space to form interconnected porous microstructure. This unique hierarchical architecture not only prevents serious restacking of graphene sheets but also allows electrolytes to diffuse freely inside and through the network. Therefore, a

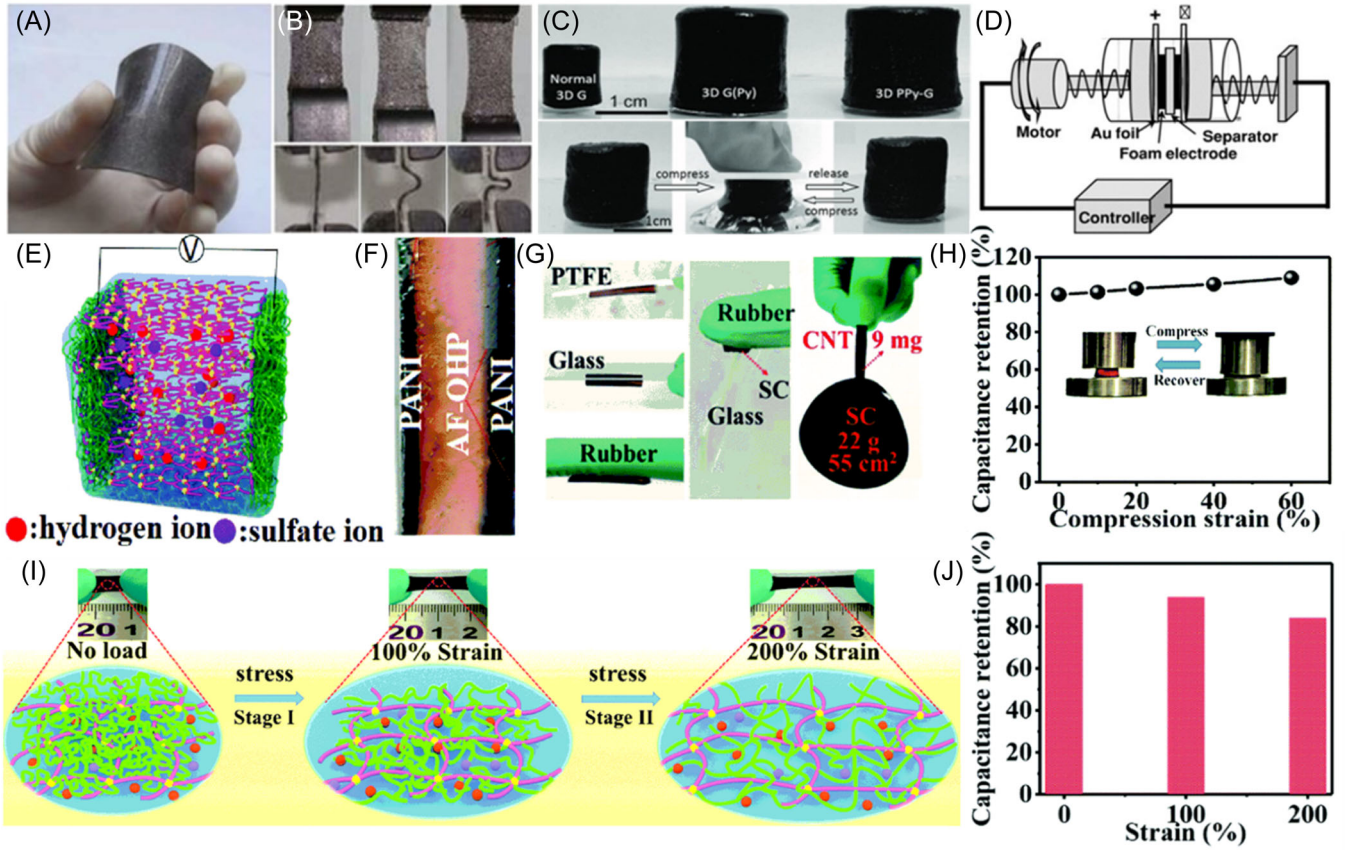

FIGURE 10 (A) Photograph of a bent graphene foam/polydimethylsiloxane (GF/PDMS) composite, showing its good flexibility. (B) The stretching and bending process of GF/PDMS. Reproduced with permission.[154] Copyright 2011, Springer Nature. Flexible PPy hydrogel-based supercapacitors: (C) EIS curve of a full cell based on symmetric electrodes. Inset: schematic of the makeup of the flexible supercapacitor. (D) CV curves of the fabricated supercapacitor under different bending conditions at a scan rate of 100 mV s^{-1}. Reproduced with permission.[161] Copyright 2013, Wiley. (E) Mechanism diagram and (F) optical picture of cross-section of AF-SSC. (G) Optical picture SCs adhered to different substrate surfaces. (H) Capacitance retention of AF-SSC under different stretch ratios of AF-SSC. (I) Schematic illustration of the stretching process. (J) Capacitance retention of AF-SSC at the current density of 0.2 mA cm^{-2} under different compress ratios. Reproduced with permission.[167] Copyright 2021, RSC. CV, cyclic voltammetry; EIS, electrochemical impendance spectroscopy.

free-standing electrode was constructed with a thickness of 3 mm graphene hydrogel supported by a gold-coated polyimide substrate. Flexible supercapacitor was assembled by using H_2SO_4-PVA as solid-state electrolyte. The change of CV curves under different bending angles at the scan rate of 10 mV s^{-1} is negligible.[160] In Figure 10C,D, the 3D hierarchically nanostructured hydrogel was synthesized by a facile interfacial polymerization method in which the polymerization is carried out at an organic/aqueous biphasic interface. The microstructure of the PPy hydrogel and its mechanical and electrochemical properties could be tuned by controlling the ratio of phytic acid to pyrrole monomers in the synthetic process.[161] Qu et al. reported a compressible supercapacitor, which is fabricated by hydrothermal treatment and electro-polymerization. The obtained PPy-G foam can sustain large-strain deformation under manual compression and recover most of the material volume. From the CV and GCD (charge and discharge) curves, the compressible supercapacitor could output stable energy with different compressive strain.[162] PANI/Ag/CNF aerogel was synthesized by situ-reduction and electrodeposition. It can deliver a capacitance of 176 mF cm^{-2}. The specific capacitance shows almost no change under different bending radii.[162] In addition, 3D electronics are mostly used in electron signaling, stimulation, and electrically triggered response devices. For bioelectronics, BSA–rGO hydrogel electrode was fabricated via photopolymerization, which is demonstrated to be a highly effective H_2O_2 biosensor electrode with low detection concentration and high sensing sensitivity after combining with hemin chloride.[163] Inspired by the adhesion behavior of mussels, a PDA-pGO-PAM multiple network hydrogel was developed, possessing high toughness and conductivity. The hydrogen-bonding and cation−π interaction between PDA

chains endow the hydrogels with self-healability and self-adhesiveness. Then the hydrogel was used as a motion sensor self-adhered on a human body to detect the electromyographic signal (EMG) during the relaxation tension of arm. And it also was cyto-compatible for regulating cell behaviors, indicating plausible therapeutic applications.[164] Jaemin demonstrated smart prosthetic skin instrumented with ultrathin, single crystalline silicon nanoribbon strain, pressure, and temperature array sensors.[150] The silicon nanoribbon (SiNR) was designed as a unique serpentine geometry to stretch according to the dynamic mechanical properties of the target skin segment. This design strategy provided the highest levels of spatio-temporal sensitivity and mechanical reliability, thereby dramatically enhancing the perception capabilities of artificial skin in response to highly variable external environments. This collection of stretchable sensors and actuators facilitates highly localized mechanical and thermal skin-like perception in response to external stimuli, thus providing unique opportunities for emerging classes of prostheses and peripheral nervous system interface technologies. To truly simulate human skin, electronic skin should be able to emulate the touch and pressure sensitivity of human skin embodying a duality of being able to recognize both medium-pressure (10–100 kPa, suitable for object manipulation) and low-pressure (<10 kPa, comparable to gentle touch) perturbations.[151] 15 nm thick layer of sputtered a-IGZO and 25 nm thick Al_2O_3 passive layer were macro machined on the top of a 1 μm thick parylene film. The transparent device exhibits a mobility of 11 $cm^2 V^{-1} s^{-1}$ and I_{on}/I_{off} greater than 10^4, which also could withstand bending radius of 50 μm and can pave the way to ultra-flexible and transparent displays. To design a concrete application, it could be used to monitor the intraocular pressure for glaucoma.[165] For human skin in robotic and prosthesis applications, slip is an important information to grab an object.[166] To address simultaneously the slip force, tactile force, and temperature, a macroscale printing fabrication technique was used to prepare a strain-engineered three-axis tactile force sensor and temperature sensor array. The flexible device can detect three-axis force, and the temperature sensitivity is ~0.25%/°C. Similarly, human skin can feel moving air without touching it physically; the device can detect the N_2 gas with a source pressure of ~0.2 MPa. Lucie[37] also prepared a soft tactile sensor using two textile electrodes, a non-stretchable copper/tin-coated textile. The flexible sensor presented minimal detectable weight and displacement is 10 mg and 8 μm within a wide normal force range (potentially up to 27 N [400 kPa]) and natural touch-like tangential force ranges from about 0.5 N to 1.8 N. Qu et al. reported a compressible supercapacitor (Figure 10E–G), which is fabricated by hydrothermal treatment and electro-polymerization. The obtained PPy-G foam can sustain large-strain deformation under manual compression and recover most of the material volume. From the CV and GCD (charge and discharge) curves, the compressible supercapacitor could output stable energy with different compressive strains.[161] Except for the compression deformation, a stretchable supercapacitor with good tackiness was fabricated based on the cross-linked PAM networks soaked by EG/Water/H_2SO_4. PANI was in situ grown onto both sides of the above organohydrogel polyelectrolyte. It warrants a high structural integrity and stable electrical conductivity under stretched states. Due to the interconnected polymer network, the external force could be evenly dissipated without causing interfacial separation between the electrode and the electrolyte (Figure 10I). As shown in Figure 10H,J, the device shows a stable energy output under bending, twisting, and stretching states.[167]

Additionally, devices that took advantage of human movement such as touching, impact, linear sliding, rotation, and vibration to produce electricity attracted much more attention.[168–176] The flexible piezoelectric thin film NG on a single thin plastic substrate converted a high-output performance of ~200 V and ~150 μA cm^{-2} from the slight mechanical deformations. The short-circuit current generated from a large-area NG (3.5 cm × 3.5 cm) reached up to ~8 μA and readily allowed more than 100 commercial blue LED arrays to operate during slight bending motions by human fingers.[169] For instance, J. M. Donelan developed a biomechanical energy harvester that generates electricity during human walking. The energy harvester mounts at the knee and selectively engages power generation at the end of the swing phase, thus assisting deceleration of the joint. When walking with one device on each leg, it produced an average of 5 W of electricity.[177]

5 | FLEXIBLE ELECTROLYTES

For batteries, liquid electrolytes have played vital roles in energy storage devices for several decades, which allow Li^+, Na^+, and K^+ to diffuse between anode and cathode. Commonly, $LiPF_6$ and NaClO4-based liquid electrolytes are used in most of the previous reports. However, liquid electrolytes are in danger of leakage and even combustion of organic electrolytes. It is also likely to induce short circuit of battery when it is assembled improperly, resulting in fire or explosion of the cells. Another disadvantage of liquid electrolytes is the inevitable alkaline metal dendrite growth in half and full cells, which is caused by uneven currents when charged in the case of porous separators. In addition, the liquid electrolyte is reducible on the anode side, and solid

electrolyte interphase is formed during the charge and discharge process, leading to the loss of ionic (e.g., Li^+, Na^+, and K^+) from the cathode and lower initial Coulombic efficiency. Replacing the organic electrolytes in different kinds of batteries with ceramic electrolyte and polymer electrolyte, which are intrinsically non-flammable, to assemble all-solid-state batteries has the promise to ultimately resolve the safety issue.

5.1 | Polymer electrolytes

Normally, a solid electrolyte should have high ionic (e.g., Li^+, Na^+, and K^+) and low electronic conductivity, wide and excellent electrochemical stability window, and chemical compatibility with the electrodes and other components of batteries. In conformity with these rules, various inorganic and polymeric electrolytes have been designed. They are generally composed of polymer matrix and liquid electrolyte and are widely used in alkaline-ion batteries owing to their excellent ionic conductivity, low rates of safety failure, and mechanical flexibility.[178] The macromolecule materials and polymerizable monomers have been used to achieve solid-state electrolyte with a certain mechanical strength.[11,179] To this end, polymer electrolytes, which integrated both the advantages of liquid electrolytes and solid electrolytes, have attracted much more attention as they can function as electrolytes and separators.

Poly (ethylene oxide) (PEO) based polymeric electrolytes have been the most extensively studied polymer systems. Wright et al. demonstrated the complexes of alkali metal ions with PEO. As known, PEO is a semicrystalline polymer whose glass transition temperature and melting point are around 60°C and 65°C, respectively. Close to the melting point, PEO becomes soft, promoting Li^+ diffusion. A lithium polymer salt (LiPSsTFSI) has been synthesized by free radical polymerization. After blending with PEO, the polymer electrolyte exhibits a high ionic conductivity of $1.35 \times 10^{-4}\,S\,cm^{-1}$ at 90°C but only $6.92 \times 10^{-5}\,S\,cm^{-1}$ at 70°C. This would be identified as the unique structure of the $-SO_2$-$N^{(-)}$-$SO(=NSO_2CF_3)$-CF_3 in the polyanion with high dissociation of Li^+ ions and enhanced the degrees of amorphous phases and the segmental motions.[180]

Besides, single Li-ion conducting solid polymer electrolytes focused on anionic centers (carboxylate [$-CO_2$], sulfonate [$-SO_3$], or sulfonylimide [$-SO_2N^{(-)}SO_2$-, $-SO_2N^{(-)}SO_2CF_3$] anions) have been investigated intensively. Particularly, weakly coordinating anions with a flexible molecular structure (e.g., bis(trifluoromethanesulfonyl)imide ([$(CF_3SO_2)_2N$], TFSI)) were primarily suggested as requisite counter anions of lithium salt. Cui et al. prepared a polymer-polymer composite electrolyte (Figure 11A,B) with nanoporous polyimide (PI) film filled with polyethylene oxide/lithium bis(trifluoromethanesulfonyl)imide (PEO/LiTFSI).[181] The PI film is incombustible and strong, preventing batteries from short-circuiting. The vertical channels with infused polymer electrolyte could enhance the ionic conductivity ($2.3 \times 10^{-4}\,S\,cm^{-1}$ at 30°C) of the composite electrolyte. The solid-state lithium-ion batteries fabricated with PI/PEO/LiTFSI solid electrolyte show good cycling performance (200 cycles at C/2 rate) at 60°C and withstand harsh tests such as bending, nail penetration, and cutting (Figure 11C–E). Other salts and polymers have been designed to resolve these problems.[182,183] For instance, Lee et al. also prepared a highly bendable plastic crystal composite electrolyte (PCCE), which is composed of UV-crosslinked ethoxylated trimethylolpropane triacrylate (ETPTA) polymer network, PVdF-HFP, and lithium bis-trifluoromethanesulfonimide in succinonitrile (Figure 11F). The S-PCCE provides excellent ionic conductivities of more than $10^{-3}\,S\,cm^{-1}$ at room temperature and strong resistance to breakage by incorporation of the UV-cured ETPTA polymer network. Notably, the S-PCCE can preserve its dimensional stability even after the 100th bending cycle (Figure 11G).[184] Wei et al. prepared a flexible all-solid-state battery with thin polyethylene glycol electrolyte, which could bend to a 1 mm radius with a capacity of $0.02\,mA\,h\,cm^{-2}$ over 100 cycles.[185] A melamine–terephthalaldehyde–lithium complex (MTF–Li) based single ion conducting electrolyte was designed as the precursor of polymer electrolyte. Then the material was blended with a PVDF–HFP binder and solution cast on a glass dish to form a single ion conducting electrolyte membrane. The tensile strength of the membrane was found to be 3.75 MPa with 31% elongation. The inherent porosity of the material facilitates the accommodation of organic solvents used in battery devices, leading to a high Li-ion mobility with an ionic conductivity in the order of $10^{-4}\,S\,cm^{-1}$ at room temperature.[186] Wang et al. also demonstrated a double network gel with liquid electrolyte. The gel electrolyte shows a conductivity of $8.1 \times 10^{-4}\,S\,cm^{-1}$ at 30°C, and it increases to above $10^{-3}\,S\,cm^{-1}$ with an increase in temperature.

In addition, several kinds of solid-state electrolytes such as PVA–KOH, cellulose–chitin–AMImBr–H_2SO_4, PVA–H_2SO_4, PMMA–EC–PC–$TEAClO_4$ and PAA–KCl, graft copolymer POEM-*g*-PDMS doped with $LiCF_3SO_3$, and poly(methyl methacrylate) networks solvated by the IL EMI.TFSI, have been reported because of high reliability without leakage of electrolyte as well as thin-form and separator-free devices.[187–190]

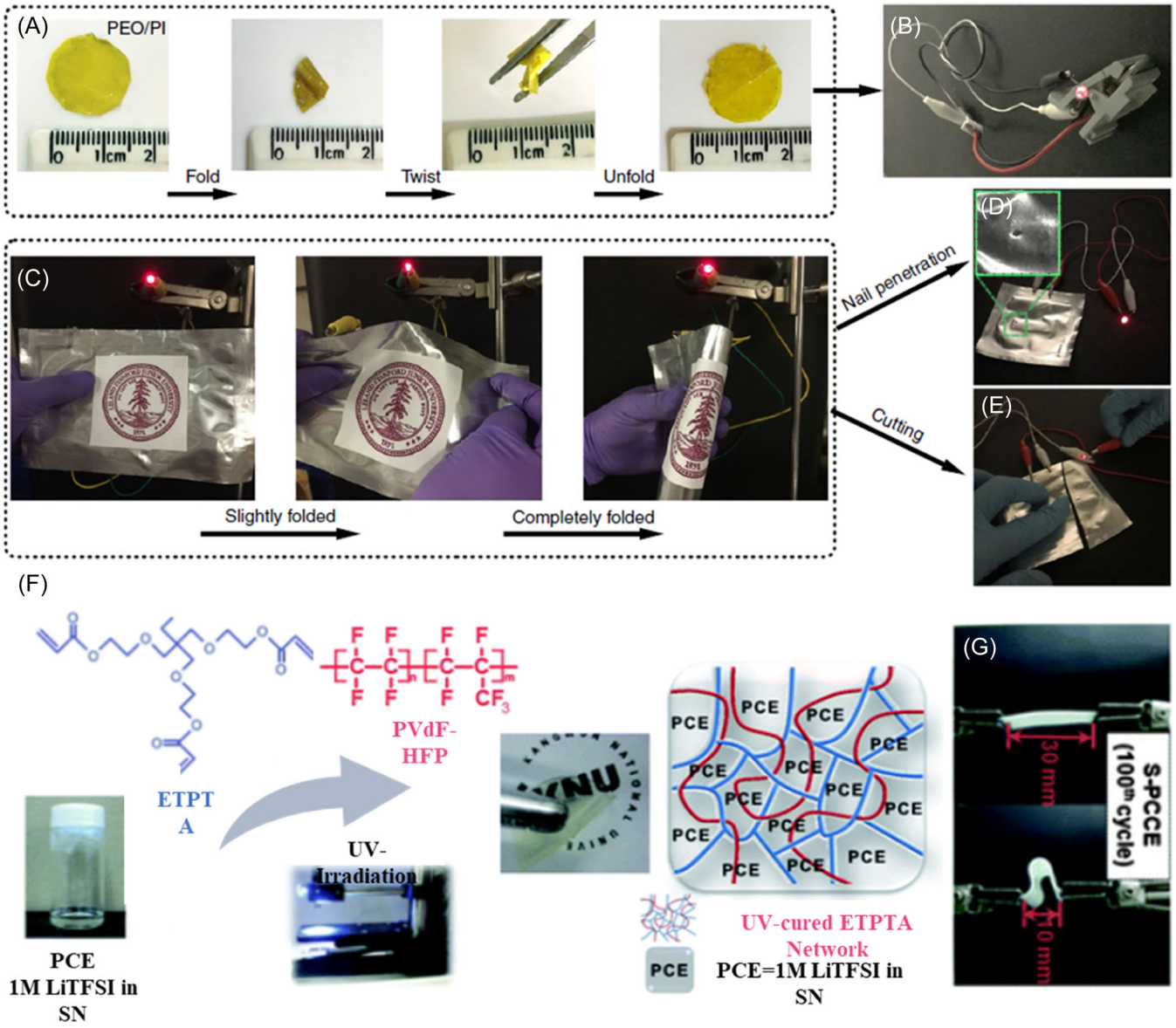

FIGURE 11 The obtained polyimide/polyethylene oxide/lithium bis(trifluoromethanesulfonyl)imide (PI/PEO/LiTFSI) polymer-polymer solid-state electrolyte (SSE). (A) Photo images of 2 cm^2 PI/PEO/LiTFSI SSE free-standing film being abused via folding, twisting, and unfolding. (B) Photo image of the abused PI/PEO/LiTFSI film as an SSE in an LFP/PI/PEO/LiTFSI/Li coin cell lighting an light-emitting diode (LED) bulb. (C) Flexible Li/PI/PEO/LiTFSI/LFP pouch cell lighting an LED bulb. (D) Li/PI/PEO/LiTFSI/LFP pouch cell lighting an LED bulb after nail test. (E) Li/PI/PEO/LiTFSI/LFP pouch cell lighting an LED bulb after cutting. Reproduced with permission.[181] Copyright 2019, Springer Nature. (F) The schematic representation illustrating the UV-curing process and photographs depicting the physical appearance of S-PCCE. (G) Mechanical bending test of S-PCCE after 100th bending cycles. Reproduced with permission.[184] Copyright 2012, RSC.

5.2 | Ceramic electrolytes

Different from the polymer electrolyte, inorganic ceramic electrolytes have high ionic conductivity (10^{-4}–10^{-3} S cm^{-1}) at ambient temperature. It also has sufficient electrochemical stability and better flame resistance. As the solid-state batteries became a research hotspot again, ceramic electrolyte has achieved significant progress.

In 2016, Kanno reported a sulfides superionic conductor with high conductivity (25 mS cm^{-1}) and stability. But the narrow electrochemical stability window, poor chemical compatibility with electrodes, and poor mechanical properties need to be settled urgently. Compared with sulfides (e.g., Li_2S–P_2S_5 and $Li_{10}GeP_2S_{12}$), ceramic oxides (e.g., $Li_7La_3Zr_2O_{12}$ and $Li_{1.3}Al_{0.3}Ti_{1.7}(PO_4)_3$) are generally more stable in ambient air and thus can be more easily

handled during processing. In particular, the garnet-type $Li_7La_3Zr_2O_{12}$ (LLZO) has attracted tremendous interest as a promising solid electrolyte due to its high ionic conductivity (about 10^{-3} S cm^{-1} at 25°C) and high chemical stability against metallic Li. Kanamura et al. obtained a flexible composite garnet-type Al-LLZO tape-by-tape casting and IL impregnation. As shown in Figure 12A, the IL can not only bond the LLZO particles, forming a lithium ions pathway, but also wet the interface of solid-state electrolyte and electrode, reducing the interface resistance. The sheet electrolyte can be casted on the PET substrate and removed easily after drying (Figure 12B,C). In the Figure 12D, the sheet electrolyte is mechanically robust and highly conductive (1×10^{-4} S cm^{-1} at 25°C).[191] With the binder of polytetrafluoroethylene (PTFE), a 3D $Li_{6.75}La_3Zr_{1.75}Ta_{0.25}O_{12}$ (LLZTO) self-supporting framework is prepared through a simple grinding method without any solvent (Figure 12E,F).[192] Subsequently, a garnet-based composite electrolyte is achieved through filling the flexible 3D LLZTO framework with a succinonitrile solid electrolyte. Due to the high content of garnet ceramic (80.4 wt.%) and high heat resistance of the PTFE binder, such a composite electrolyte film with nonflammability and high processability exhibits a wide electrochemical window of 4.8 V versus Li/Li$^+$ and high ionic transference number of 0.53. The continuous Li$^+$ transfer channels between interconnected LLZTO particles and succinonitrile and the soft electrolyte/electrode interface jointly contribute to a high ambient-temperature ionic conductivity of 1.2×10^{-4} S cm^{-1} and excellent long-term stability of the Li symmetric battery.

5.3 | Polymer and ceramic hybrid electrolytes

Hybrid electrolytes possess the merit of polymer electrolytes, and inorganic ceramic electrolytes exhibit comparable ionic conductivity, high mechanical strength, and favorable interfacial contact with electrodes, which greatly improve the electrochemical performance of all-solid-state batteries.[193] It is significant to integrate

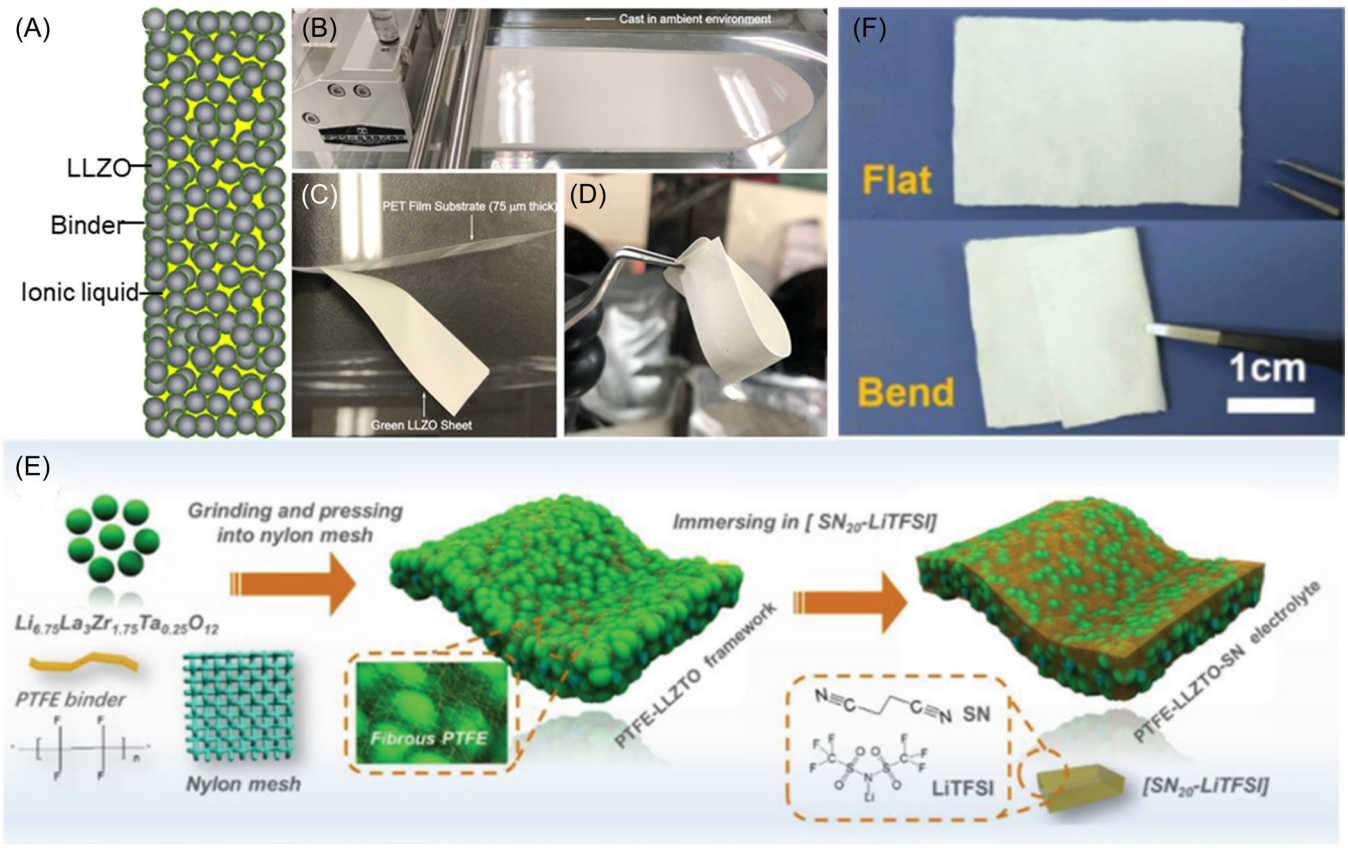

FIGURE 12 Concept of the flexible composite Al-LLZO sheet electrolyte and its synthesis at room temperature. (A) Illustration of the composite sheet electrolyte, (B) doctor-blade casting of the sheet electrolyte in ambient air, (C) As-cast green sheet, and (D) cold-pressed and IL-impregnated Al-LLZO sheet electrolyte. Reproduced with permission.[191] Copyright 2020, ACS. (E) The preparation schematic of 5PTFE-100LLZTO-16[SN20−LiTFSI] electrolyte. (F) Flat and bend state of 5PTFE-100LLZTO-16[SN20−LiTFSI] electrolyte. Reproduced with permission.[192] Copyright 2020, Wiley.

ceramic electrolyte with polymer electrolyte to endow electrolytes with high ionic conductivity and good mechanical properties, creating "ceramic in polymer" (CIP) or "polymer in ceramic" (PIC) materials.

The ceramic particle fillers are dispersed into the polymer matrix to enhance ionic conductivity. A sandwich-type composite electrolyte was fabricated by a PIC-5 μm interlayer sandwiched between two CIP-200 nm thin layers. The effect of various content and different particle sizes of LLZTO on the conductivity was investigated. Cui and his coworkers demonstrated that 15 wt.% $Li_{0.33}La_{0.557}TiO_3$ nanowire was dispersed in polyacrylonitrile-$LiClO_4$, which exhibits an unprecedented ionic conductivity of 2.4×10^{-4} S cm^{-1} at room temperature, suggesting that ceramic nanowire fillers can facilitate the formation of ionic conduction networks in polymer-based solid electrolyte. In addition, the composite electrolyte also shows an enlarged electrochemical stability window in comparison to the one without fillers. The discovery paves the way for the design of solid ion electrolytes with superior performance.[194] In Figure 13A,B, a 30–50 μm thickness flexible LLZO-PEO ($LiClO_4$) composite electrolyte was prepared by solution-casting method. The Li ions pathway was investigated systematically. The Li ions mainly pass through LLZO ceramic particles, not the interface or the PEO polymer.[195] John B. Goodenough and his coworkers also designed a CPMEA/LATP/CPMEA sandwich electrolyte. In the architecture, the ceramic layer (LATP) can block anion transport, which reduces the double-layer electric field at the Li/polymer interface and the decomposition of the polymer electrolyte to improve the Coulombic efficiency of a device. The polymer electrolyte layer, which is in direct contact with electrodes, can suppress dendrite nucleation due to the uniform Li^+ flux on the polymer/lithium interface and better wetting ability toward lithium metal.[196] With the PEO as the binder, an ionic liquid (BMP-TFSI) modified flexible concrete structured composite solid electrolyte membrane was obtained (Figure 13C). The as-prepared membrane is free-standing and exhibits excellent ductility and flexibility.

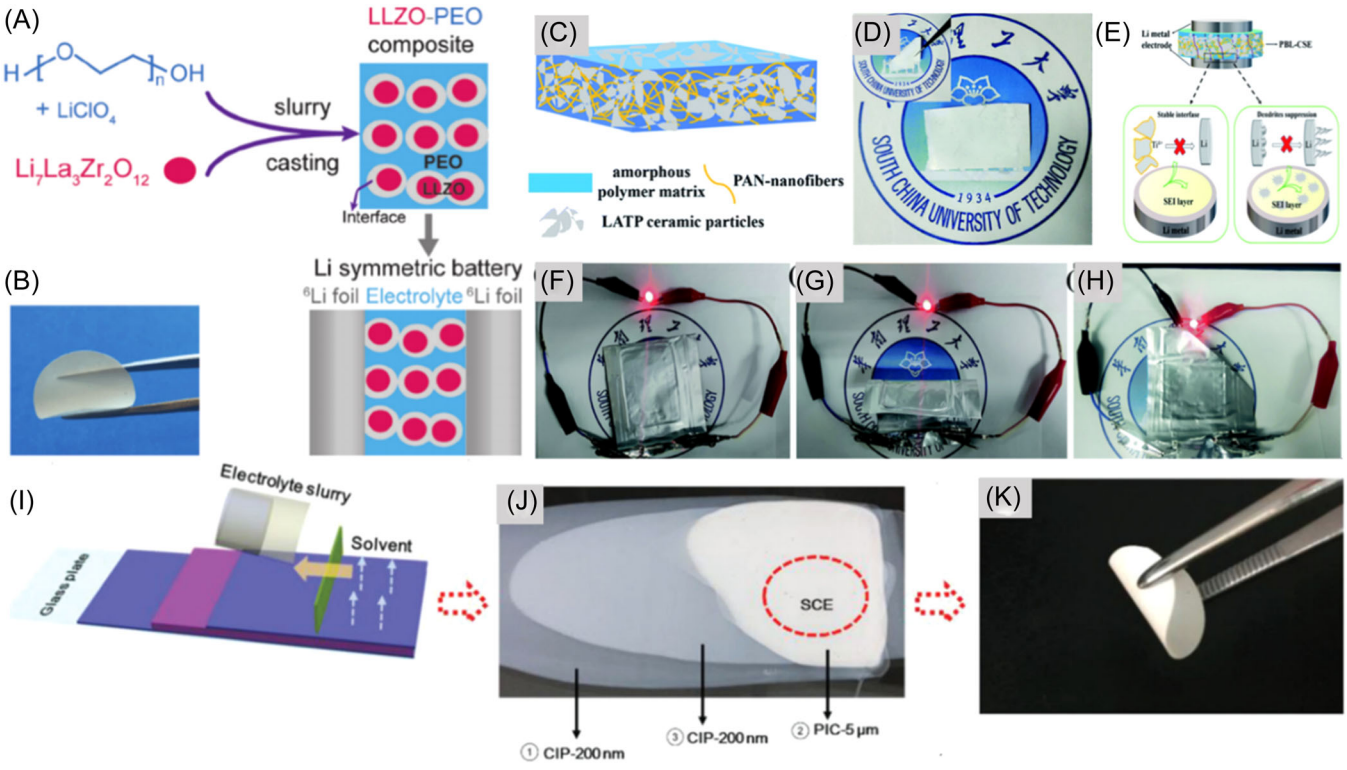

FIGURE 13 (A) Illustration of the process for preparing LLZO-PEO composite electrolytes. (B) Picture of the as-synthesized flexible composite electrolyte. Reproduced with permission.[195] Copyright 2020, Wiley. (C) Schematic illustration of the structure and Li-ion transport mechanism of the PBL-CSE membrane. (D) Digital photograph of the PBL-CSE membrane in the unfolded and bent state (inset). (E) The schematic illustration for the mechanism behind the outstanding Li dendrite suppression ability and superior interface stability against Li metal. (F) Images of the flexible $LiFePO_4$/PBL-CSE/Li pouch Li metal cell lighting an light-emitting diode bulb even with folding (G) and the corner cut off (H). Reproduced with permission.[199] Copyright 2020, RSC. (I) The schematic illustration of the SCE preparation by blade casting. Digital images of as-casted SCE on a glass plate (J) and the bendable SCE (K). Reproduced with permission.[200] Copyright 2020, Wiley.

No cracks could be found in the electrolyte films upon bending, indicating an excellent mechanical capability (Figure 13D). The addition of the ionic liquid (BMP-TFSI) can not only improve the ionic conductivity but also enhance the interface stability, suppressing the Li dendrite growth (Figure 13E). With the PBL-CSE membrane used as a separator, the solid-state pouch cell presented greatly improved electrochemical performance, thermal stability, and good compatibility toward the Li metal electrode. It can light up a red light-emitting diode (LED) even with folded and corner cut off (Figure 13F–H). The effect of particle size and concentration on the strength, ionic conductivity, and interfacial flexibility of composite electrolyte was also investigated. In Figure 13I,J, a sandwich-type composite electrolyte was fabricated by blade casting with a mechanically strong PIC interlayer and flexible CIP outer layer. Such SCE achieves both excellent lithium dendrite suppression and interfacial contact with Li metal (Figure 13K). Except above active filler (e.g., Li_3N[197] and $Li_{1.3}Al_{0.3}Ti_{1.7}(PO_4)_3$[198]), inactive fillers such as Al_2O_3 have been widely used.

6 | CONCLUSION AND OUTLOOK

In summary, flexible rechargeable batteries, SCs, nanogenerators, and bioelectronics have been assembled to get robust mechanical stability under frequent mechanical strain, while maintaining excellent electrochemical performance. However, numerous technical challenges still hinder the development of the flexible devices. A new concept of electronic devices will be designed to meet the mechanical flexibility requirement. The wire or planar structure with omnidirectional flexibility (e.g., stretch, twisting, compress, and bend) is identified as a promising unit, which can be weaved into fabric, facilitating the rapid growth of wearable electronics.[201,202]

For flexible battery, the flexibility of each component is critical for the development of high-performance flexible devices. For electrodes, great progress has been made on high-capacity anode materials. But flexible cathode materials based on $LiCoO_2$, $LiMn_2O_4$, $LiNi_{1/3}Mn_{1/3}Co_{1/3}O_2$, and so forth, are rarely reported. Therefore, the next stage for flexible electrode will mostly focus

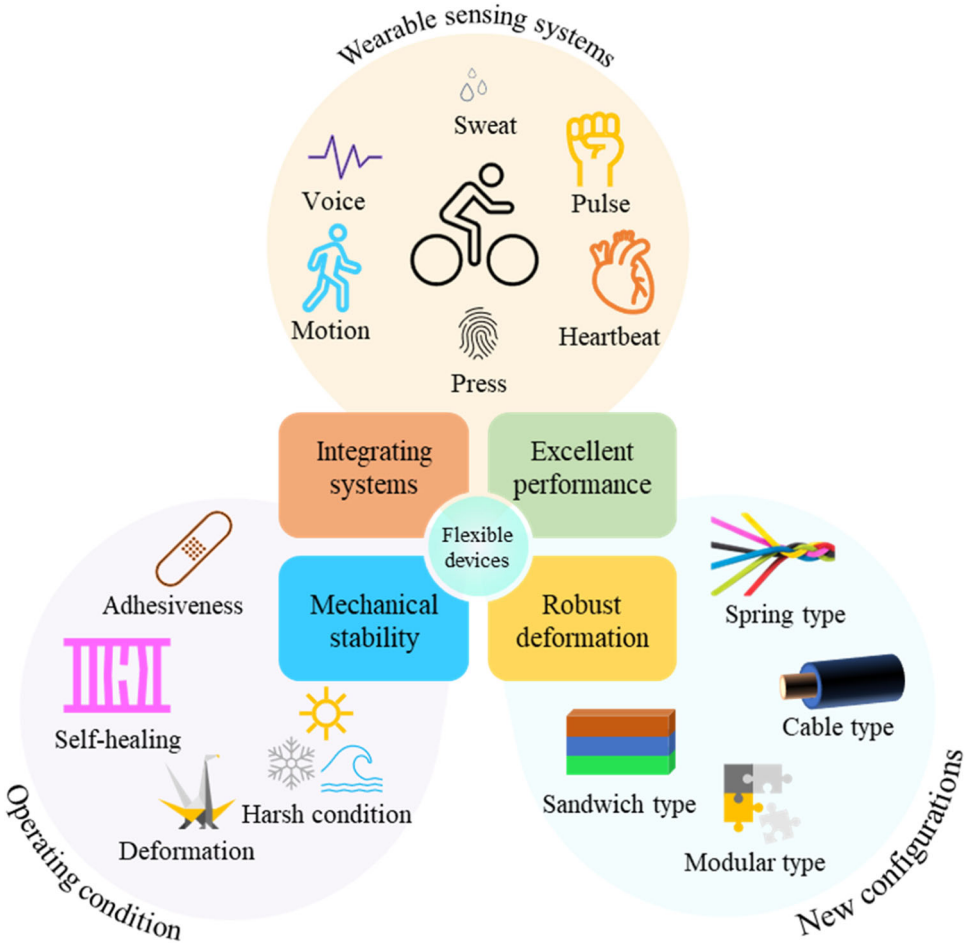

FIGURE 14 Development perspectives on flexible wearable electronics.

on flexible cathode material. Much more effort will be devoted to flexible lithium-ion and sodium-ion batteries. In terms of the flexible electrolyte, the development of solid-state electrolytes with higher ionic conductivity and larger operating voltage windows is a significant trend in the future. The interface between electrolytes and electrodes should pay more attention because of the different elastic modulus of the electrolytes and electrodes. To get a stable interface between electrolyte and electrodes, a composite electrolyte (CIP or PIC) should be designed with excellent interfacial flexibility and high ionic conductivity. And it not only can suppress the growth of Li dendrite but also can suppress the growth of Li dendrite.

For skin-like devices, polymeric supporting layers should form intimate and robust contact with skin via van der Waals forces. As shown in Figure 14, different kinds of sensors (humidity sensor, temperature sensor, airflow sensor, and so forth), wireless power, and communication system are integrated on skin or skin-friendly polymer substrate to digitize biological signals and monitor basic healthcare. And these soft, miniaturized, wireless, and integrated devices will apply for diagnosis to advanced human–machine interfaces and therapeutics, offering infinite options for on-skin and implantable human–machine interaction.

In terms of application, the innovational configurations, including fiber structure (coaxial, twisting, parallel, and rolling structure), layer structure (sandwich-type and laminated), and all-in-one structure, will be developed by spinning, thermal drawing, 3D printing, surface coating, and other techniques. The fiber- and layer-type devices are easy to be woven into cloth, while the all-in-one structure can avoid the mechanical mismatches between electrodes and electrolytes. Due to the sliding and delamination under large deformations, it is necessary and essential to develop new configurations and materials for flexible electronic devices, which can render a stable signal output with large and complex deformation under water, low temperature, and other extreme conditions.

To further insight into the performance with complicated deformation, advanced simulation methods should be used to build the connection between the mechanical and electrochemical performance and understand the mass transport and electrochemical processes related to the flexible batteries under external mechanical forces, which is critical to the rational design of new configurations with high performance and flexibility.

ACKNOWLEDGMENTS

Qi Zhang and Xuan-Wen Gao make an equal contribution to this work. This work was supported by the National Natural Science Foundation of China (Grant Nos. 52272194 and 32301542), the LiaoNing Revitalization Talents Program (Grant No. XLYC2007155), and the Fundamental Research Program of Shanxi Province (No. 20210302123109; 20210302124426). This manuscript was written through the contributions of all the authors. All authors have approved the final version of the manuscript.

CONFLICT OF INTEREST STATEMENT

The authors declare no conflict of interest.

ORCID

Qi Zhang https://orcid.org/0000-0002-3846-9395
Wen-Bin Luo https://orcid.org/0000-0002-9886-5461

REFERENCES

1. Nomura K, Ohta H, Takagi A, Kamiya T, Hirano M, Hosono H. Room-temperature fabrication of transparent flexible thin-film transistors using amorphous oxide semiconductors. *Nature*. 2004;432:488-492.
2. Gustafsson G, Cao Y, Treacy GM, Klavetter F, Colaneri N, Heeger AJ. Flexible light-emitting diodes made from soluble conducting polymers. *Nature*. 1992;357:477-479.
3. Kaltenbrunner M, White MS, Głowacki ED, et al. Ultrathin and lightweight organic solar cells with high flexibility. *Nat Commun*. 2012;3:770.
4. Fan Q, Miao J, Liu X, et al. Biomimetic hierarchically silver nanowire interwoven MXene mesh for flexible transparent electrodes and invisible camouflage electronics. *Nano Lett*. 2022;22:740-750.
5. Shen L, Lan G, Lu L, et al. Flexible devices: a strategy to modulate the bending coupled microwave magnetism in nanoscale epitaxial lithium ferrite for flexible spintronic devices. *Adv Sci*. 2018;5:1870077.
6. Liu Y, He K, Chen G, Leow WR, Chen X. Nature-inspired structural materials for flexible electronic devices. *Chem Rev*. 2017;117:12893-12941.
7. Gaikwad AM, Zamarayeva AM, Rousseau J, Chu H, Derin I, Steingart DA. Highly stretchable alkaline batteries based on an embedded conductive fabric. *Adv Mater*. 2012;24:5071-5076.
8. Yousaf M, Shi HTH, Wang Y, et al. Novel pliable electrodes for flexible electrochemical energy storage devices: recent progress and challenges. *Adv Energy Mater*. 2016;6:1600490.
9. Nyström G, Razaq A, Strømme M, Nyholm L, Mihranyan A. Ultrafast all-polymer paper-based batteries. *Nano Lett*. 2009;9:3635-3639.
10. Bouchet R, Maria S, Meziane R, et al. Single-ion BAB triblock copolymers as highly efficient electrolytes for lithium-metal batteries. *Nat Mater*. 2013;12:452-457.
11. Croce F, Appetecchi GB, Persi L, Scrosati B. Nanocomposite polymer electrolytes for lithium batteries. *Nature*. 1998;394:456-458.
12. Dang H, Wang B, Chang Z, et al. Recycled lithium from simulated pyrometallurgical slag by chlorination roasting. *ACS Sustain Chem Eng*. 2018;6:13160-13167.
13. Fang X, Weng W, Ren J, Peng H. A cable-shaped lithium sulfur battery. *Adv Mater*. 2016;28:491-496.
14. Wahyudi W, Cao Z, Kumar P, et al. Phase inversion strategy to flexible freestanding electrode: critical coupling of binders

and electrolytes for high performance Li–S battery. *Adv Funct Mater*. 2018;28:1802244.

15. Kumar KS, Choudhary N, Jung Y, Thomas J. Recent advances in two-dimensional nanomaterials for supercapacitor electrode applications. *ACS Energy Lett*. 2018;3:482-495.
16. Fan L, Lin K, Wang J, Ma R, Lu B. A nonaqueous potassium-based battery–supercapacitor hybrid device. *Adv Mater*. 2018;30:1800804.
17. Strauss V, Marsh K, Kowal MD, El-Kady M, Kaner RB. A simple route to porous graphene from carbon nanodots for supercapacitor applications. *Adv Mater*. 2018;30:1704449.
18. Hu Y, Ye D, Luo B, et al. A binder-free and free-standing cobalt sulfide@Carbon nanotube cathode material for aluminum-ion batteries. *Adv Mater*. 2018;30:1703824.
19. Sun D, Zhu X, Luo B, et al. New binder-free metal phosphide–carbon felt composite anodes for sodium-ion battery. *Adv Energy Mater*. 2018;8:1801197.
20. Zhao W, Ding M, Guo L, Yang HY. Dual-Ion electrochemical deionization system with binder-free aerogel electrodes. *Small*. 2019;15:1805505.
21. Zhou Y, Maleski K, Anasori B, et al. $Ti_3C_2T_x$ MXene-reduced graphene oxide composite electrodes for stretchable supercapacitors. *ACS Nano*. 2020;14:3576-3586.
22. Wang P, Chen Z, Wang H, et al. A high-performance flexible aqueous Al ion rechargeable battery with long cycle life. *Energy Storage Mater*. 2020;25:426-435.
23. Orangi J, Hamade F, Davis VA, Beidaghi M. 3D printing of additive-free 2D $Ti_3C_2T_x$ (MXene) ink for fabrication of micro-supercapacitors with ultra-high energy densities. *ACS Nano*. 2020;14:640-650.
24. Chen W, Zhang X, Mi L, et al. High-performance flexible freestanding anode with hierarchical 3D carbon-networks/Fe_7S_8/graphene for applicable sodium-ion batteries. *Adv Mater*. 2019;31:1806664.
25. Wang X, Zhang Y, Zhang X, et al. A highly stretchable transparent self-powered triboelectric tactile sensor with metallized nanofibers for wearable electronics. *Adv Mater*. 2018;30:1706738.
26. Zhang Q, Gao X-W, Shi Y, et al. Electrocatalytic-driven compensation for sodium ion pouch cell with high energy density and long lifespan. *Energy Storage Mater*. 2021;39:54-59.
27. Li H, Liu Z, Liang G, et al. Waterproof and tailorable elastic rechargeable yarn zinc ion batteries by a cross-linked polyacrylamide electrolyte. *ACS Nano*. 2018;12:3140-3148.
28. Zhang C, Kremer MP, Seral-Ascaso A, et al. Stamping of flexible, coplanar micro-supercapacitors using MXene inks. *Adv Funct Mater*. 2018;28:1705506.
29. Zhang J, Zang X, Wen H, et al. High-voltage and free-standing poly(propylene carbonate)/$Li_{6.75}La_3Zr_{1.75}Ta_{0.25}O_{12}$ composite solid electrolyte for wide temperature range and flexible solid lithium-ion battery. *J Mater Chem A*. 2017;5:4940-4948.
30. Deng Z, Jiang H, Hu Y, et al. 3D ordered macroporous MoS_2@C nanostructure for flexible Li-ion batteries. *Adv Mater*. 2017;29:1603020.
31. Liu Z, Wu Z-S, Yang S, Dong R, Feng X, Müllen K. Ultraflexible in-plane micro-supercapacitors by direct printing of solution-processable electrochemically exfoliated graphene. *Adv Mater*. 2016;28:2217-2222.
32. Fu K, Gong Y, Dai J, et al. Flexible, solid-state, ion-conducting membrane with 3D garnet nanofiber networks for lithium batteries. *Proc Natl Acad Sci*. 2016;113:7094-7099.
33. Meng F, Zhong H, Bao D, Yan J, Zhang X. In situ coupling of strung Co_4N and intertwined N–C fibers toward free-standing bifunctional cathode for robust, efficient, and flexible Zn–Air batteries. *J Am Chem Soc*. 2016;138:10226-10231.
34. Schmidt TM, Larsen-Olsen TT, Carlé JE, Angmo D, Krebs FC. Upscaling of perovskite solar cells: fully ambient roll processing of flexible perovskite solar cells with printed back electrodes. *Adv Energy Mater*. 2015;5:1500569.
35. Hyun WJ, Secor EB, Hersam MC, Frisbie CD, Francis LF. High-resolution patterning of graphene by screen printing with a silicon stencil for highly flexible printed electronics. *Adv Mater*. 2015;27:109-115.
36. Wang G, Wang H, Lu X, et al. Solid-state supercapacitor based on activated carbon cloths exhibits excellent rate capability. *Adv Mater*. 2014;26:2676-2682.
37. Viry L, Levi A, Totaro M, et al. Flexible three-axial force sensor for soft and highly sensitive artificial touch. *Adv Mater*. 2014;26:2659-2664.
38. Liu J, Chen M, Zhang L, et al. A flexible alkaline rechargeable Ni/Fe battery based on graphene Foam/Carbon nanotubes hybrid film. *Nano Lett*. 2014;14:7180-7187.
39. Amjadi M, Pichitpajongkit A, Lee S, Ryu S, Park I. Highly stretchable and sensitive strain sensor based on silver nanowire–elastomer nanocomposite. *ACS Nano*. 2014;8:5154-5163.
40. Le VT, Kim H, Ghosh A, et al. Coaxial fiber supercapacitor using all-carbon material electrodes. *ACS Nano*. 2013;7:5940-5947.
41. Xu Y, Lin Z, Huang X, Wang Y, Huang Y, Duan X. Functionalized graphene hydrogel-based high-performance supercapacitors. *Adv Mater*. 2013;25:5779-5784.
42. Meng Y, Zhao Y, Hu C, et al. All-graphene core-sheath microfibers for all-solid-state, stretchable fibriform supercapacitors and wearable electronic textiles. *Adv Mater*. 2013;25:2326-2331.
43. He Y, Chen W, Li X, et al. Freestanding three-dimensional Graphene/MnO_2 composite networks as ultralight and flexible supercapacitor electrodes. *ACS Nano*. 2013;7:174-182.
44. Li N, Chen Z, Ren W, Li F, Cheng HM. Flexible graphene-based lithium-ion batteries with ultrafast charge and discharge rates. *Proc Natl Acad Sci*. 2012;109:17360-17365.
45. Fan F-R, Lin L, Zhu G, Wu W, Zhang R, Wang ZL. Transparent triboelectric nanogenerators and self-powered pressure sensors based on micropatterned plastic films. *Nano Lett*. 2012;12:3109-3114.
46. Yuan L, Lu X-H, Xiao X, et al. Flexible solid-state supercapacitors based on carbon nanoparticles/MnO_2 nanorods hybrid structure. *ACS Nano*. 2012;6:656-661.
47. El-Kady MF, Strong V, Dubin S, Kaner RB. Laser scribing of high-performance and flexible Graphene-Based electrochemical capacitors. *Science*. 2012;335:1326-1330.
48. Yun YJ, Hong WG, Kim W-J, Jun Y, Kim BH. A novel method for applying reduced graphene oxide directly to electronic textiles from yarns to fabrics. *Adv Mater*. 2013;25:5701-5705.
49. Zhang W, Miao J, Zuo X, Zhang X, Qu L. Weaving a magnificent world: 1D fibrous electrodes and devices for stretchable and wearable electronics. *J Mater Chem C*. 2022;10:14027-14052.

50. Zhu S, So J-H, Mays R, et al. Ultrastretchable fibers with metallic conductivity using a liquid metal alloy core. *Adv Funct Mater*. 2013;23:2308-2314.
51. Xu Z, Sun H, Zhao X, Gao C. Ultrastrong fibers assembled from giant graphene oxide sheets. *Adv Mater*. 2013;25:188-193.
52. Zuo X, Fan T, Qu L, Zhang X, Miao J. Smart multi-responsive aramid aerogel fiber enabled self-powered fabrics. *Nano Energy*. 2022;101:107559.
53. Zuo X, Zhang X, Qu L, Miao J. Smart fibers and textiles for personal thermal management in emerging wearable applications. *Adv. Mater. Technol*. 2023;8:2201137.
54. Ren J, Zhang Y, Bai W, et al. Elastic and wearable wire-shaped lithium-ion battery with high electrochemical performance. *Angew Chem*. 2014;126:7998-8003.
55. Lin H, Weng W, Ren J, et al. Twisted aligned carbon nanotube/silicon composite fiber anode for flexible wire-shaped lithium-ion battery. *Adv Mater*. 2014;26:1217-1222.
56. Sun C-F, Zhu H, Baker Iii EB, et al. Weavable high-capacity electrodes. *Nano Energy*. 2013;2:987-994.
57. Weng W, Sun Q, Zhang Y, et al. Winding aligned carbon nanotube composite yarns into coaxial fiber full batteries with high performances. *Nano Lett*. 2014;14:3432-3438.
58. Zhang Y, Bai W, Cheng X, et al. Flexible and stretchable lithium-ion batteries and supercapacitors based on electrically conducting carbon nanotube fiber springs. *Angew Chem, Int Ed*. 2014;53:14564-14568.
59. Zhang Y, Bai W, Ren J, et al. Super-stretchy lithium-ion battery based on carbon nanotube fiber. *J Mater Chem A*. 2014;2:11054-11059.
60. Miao J, Fan T. Flexible and stretchable transparent conductive graphene-based electrodes for emerging wearable electronics. *Carbon*. 2023;202:495-527.
61. Zhou Y, Wang C-H, Lu W, Dai L. Recent advances in fiber-shaped supercapacitors and lithium-ion batteries. *Adv Mater*. 2020;32:1902779.
62. Wang L, Fu X, He J, et al. Application challenges in fiber and textile electronics. *Adv Mater*. 2020;32:1901971.
63. Chen D, Jiang K, Huang T, Shen G. Recent advances in fiber supercapacitors: materials, device configurations, and applications. *Adv Mater*. 2020;32:1901806.
64. Dong Z, Jiang C, Cheng H, et al. Facile fabrication of light, flexible and multifunctional graphene fibers. *Adv Mater*. 2012;24:1856-1861.
65. Cheng H, Liu J, Zhao Y, et al. Graphene fibers with predetermined deformation as moisture-triggered actuators and robots. *Angew Chem, Int Ed*. 2013;52:10482-10486.
66. Cheng H, Hu Y, Zhao F, et al. Moisture-activated torsional graphene-fiber motor. *Adv Mater*. 2014;26:2909-2913.
67. Yang Z, Sun H, Chen T, Qiu L, Luo Y, Peng H. Photovoltaic wire derived from a graphene composite fiber achieving an 8.45% energy conversion efficiency. *Angew Chem, Int Ed*. 2013;52:7545-7548.
68. Xu Z, Liu Z, Sun H, Gao C. Highly electrically conductive Ag-doped graphene fibers as stretchable conductors. *Adv Mater*. 2013;25:3249-3253.
69. Yu J, Lu W, Smith JP, et al. A high performance stretchable asymmetric fiber-shaped supercapacitor with a core-sheath helical structure. *Adv Energy Mater*. 2017;7:1600976.
70. Wen Z, Yeh M-H, Guo H, et al. Self-powered textile for wearable electronics by hybridizing fiber-shaped nanogenerators, solar cells, and supercapacitors. *Sci Adv*. 2016;2:e1600097.
71. Bae J, Song MK, Park YJ, Kim JM, Liu M, Wang ZL. Fiber supercapacitors made of nanowire-fiber hybrid structures for wearable/flexible energy storage. *Angew Chem, Int Ed*. 2011;50:1683-1687.
72. Zheng X, Yao L, Qiu Y, Wang S, Zhang K. Core–sheath porous polyaniline nanorods/graphene fiber-shaped supercapacitors with high specific capacitance and rate capability. *ACS Appl Energy Mater*. 2019;2:4335-4344.
73. Wang S, Liu N, Su J, et al. Highly stretchable and self-healable supercapacitor with reduced graphene oxide based fiber springs. *ACS Nano*. 2017;11:2066-2074.
74. Keum K, Lee G, Lee H, et al. Wire-shaped supercapacitors with organic electrolytes fabricated via layer-by-layer assembly. *ACS Appl Mater Interfaces*. 2018;10:26248-26257.
75. Dong X, Guo Z, Song Y, et al. Flexible and wire-shaped micro-supercapacitor based on $Ni(OH)_2$-nanowire and ordered mesoporous carbon electrodes. *Adv Funct Mater*. 2014;24:3405-3412.
76. Pu X, Li L, Liu M, et al. Wearable self-charging power textile based on flexible yarn supercapacitors and fabric nanogenerators. *Adv Mater*. 2016;28:98-105.
77. Huang Y, Ip WS, Lau YY, et al. Weavable, conductive Yarn-Based NiCo//Zn textile battery with high energy density and rate capability. *ACS Nano*. 2017;11:8953-8961.
78. Chong WG, Huang J-Q, Xu Z-L, Qin X, Wang X, Kim JK. Lithium–sulfur battery cable made from ultralight, flexible graphene/carbon nanotube/sulfur composite fibers. *Adv Funct Mater*. 2017;27:1604815.
79. Kwon YH, Woo S-W, Jung H-R, et al. Cable-type flexible lithium ion battery based on hollow multi-helix electrodes. *Adv Mater*. 2012;24:5192-5197.
80. Zhu Y-H, Yuan, S, Bao D, et al. Decorating waste cloth via industrial wastewater for tube-type flexible and wearable sodium-ion batteries. *Adv Mater*. 2017;29:1603719.
81. Chen Q, Sun S, Zhai T, Yang M, Zhao X, Xia H. Yolk–shell NiS_2 nanoparticle-embedded carbon fibers for flexible fiber-shaped sodium battery. *Adv Energy Mater*. 2018;8:1800054.
82. Sun H, You X, Deng J, et al. Novel graphene/carbon nanotube composite fibers for efficient Wire-Shaped miniature energy devices. *Adv Mater*. 2014;26:2868-2873.
83. Zhang Z, Chen X, Chen P, et al. Integrated polymer solar cell and electrochemical supercapacitor in a flexible and stable fiber format. *Adv Mater*. 2014;26:466-470.
84. Wang J, Li X, Zi Y, et al. A flexible fiber-based supercapacitor–triboelectric-nanogenerator power system for wearable electronics. *Adv Mater*. 2015;27:4830-4836.
85. Dong K, Wang Y-C, Deng J, et al. A highly stretchable and washable all-yarn-based self-charging knitting power textile composed of fiber triboelectric nanogenerators and supercapacitors. *ACS Nano*. 2017;11:9490-9499.
86. Liu F, Song S, Xue D, Zhang H. Folded structured graphene paper for high performance electrode materials. *Adv Mater*. 2012;24:1089-1094.
87. Gwon H, Kim H-S, Lee KU, et al. Flexible energy storage devices based on graphene paper. *Energy Environ Sci*. 2011;4:1277-1283.

88. Meng Y, Wang K, Zhang Y, Wei Z. Hierarchical porous graphene/polyaniline composite film with superior rate performance for flexible supercapacitors. *Adv Mater*. 2013;25:6985-6990.
89. Pushparaj VL, Shaijumon MM, Kumar A, et al. Flexible energy storage devices based on nanocomposite paper. *Proc Natl Acad Sci*. 2007;104:13574-13577.
90. Hu L, Wu H, La Mantia F, Yang Y, Cui Y. Thin, flexible secondary Li-ion paper batteries. *ACS Nano*. 2010;4:5843-5848.
91. Xiao X, Peng X, Jin H, et al. Freestanding mesoporous VN/CNT hybrid electrodes for flexible all-solid-state supercapacitors. *Adv Mater*. 2013;25:5091-5097.
92. Wang H, Cui L-F, Yang Y, et al. Mn_3O_4–Graphene hybrid as a high-capacity anode material for lithium ion batteries. *J Am Chem Soc*. 2010;132:13978-13980.
93. Wang D, Choi D, Li J, et al. Self-assembled TiO_2–graphene hybrid nanostructures for enhanced Li-ion insertion. *ACS Nano*. 2009;3:907-914.
94. Paek S-M, Yoo E, Honma I. Enhanced cyclic performance and lithium storage capacity of SnO_2/graphene nanoporous electrodes with three-dimensionally delaminated flexible structure. *Nano Lett*. 2009;9:72-75.
95. Wu J, Gao X, Yu H, et al. A scalable free-standing V_2O_5/CNT film electrode for supercapacitors with a wide operation voltage (1.6 V) in an aqueous electrolyte. *Adv Funct Mater*. 2016;26:6114-6120.
96. Shin WH, Jeong HM, Kim BG, Kang JK, Choi JW. Nitrogen-doped multiwall carbon nanotubes for lithium storage with extremely high capacity. *Nano Lett*. 2012;12:2283-2288.
97. Reddy ALM, Srivastava A, Gowda SR, Gullapalli H, Dubey M, Ajayan PM. Synthesis of nitrogen-doped graphene films for lithium battery application. *ACS Nano*. 2010;4:6337-6342.
98. Aricò AS, Bruce P, Scrosati B, Tarascon JM, van Schalkwijk W. Nanostructured materials for advanced energy conversion and storage devices. *Nat Mater*. 2005;4:366-377.
99. Liu B, Zhang J, Wang X, et al. Hierarchical three-dimensional $ZnCo_2O_4$ nanowire arrays/carbon cloth anodes for a novel class of high-performance flexible lithium-ion batteries. *Nano Lett*. 2012;12:3005-3011.
100. Jia X, Chen Z, Suwarnasarn A, et al. High-performance flexible lithium-ion electrodes based on robust network architecture. *Energy Environ Sci*. 2012;5:6845-6849.
101. David L, Bhandavat R, Singh G. MoS_2/graphene composite paper for sodium-ion battery electrodes. *ACS Nano*. 2014;8:1759-1770.
102. Liu Y, Fang Y, Zhao Z, Yuan C, Lou XW. A ternary $Fe_{1-x}S$@Porous carbon nanowires/reduced graphene oxide hybrid film electrode with superior volumetric and gravimetric capacities for flexible sodium ion batteries. *Adv Energy Mater*. 2019;9:1803052.
103. Zhu Y-H, Yang X, Bao D, et al. High-energy-density flexible potassium-ion battery based on patterned electrodes. *Joule*. 2018;2:736-746.
104. Choi J-Y, Lee DJ, Lee YM, et al. Silicon nanofibrils on a flexible current collector for bendable lithium-ion battery anodes. *Adv Funct Mater*. 2013;23:2108-2114.
105. Zhao X, Hayner CM, Kung MC, Kung HH. In-plane vacancy-enabled high-power Si–graphene composite electrode for lithium-ion batteries. *Adv Energy Mater*. 2011;1:1079-1084.
106. Lee JK, Smith KB, Hayner CM, Kung HH. Silicon nanoparticles–graphene paper composites for li ion battery anodes. *Chem Commun*. 2010;46:2025-2027.
107. Zhang H, Jing S, Hu Y, Jiang H, Li C. A flexible freestanding Si/rGO hybrid film anode for stable Li-ion batteries. *J Power Sources*. 2016;307:214-219.
108. Liu J, Guan C, Zhou C, et al. A flexible quasi-solid-state nickel–zinc battery with high energy and power densities based on 3D electrode design. *Adv Mater*. 2016;28:8732-8739.
109. Li C, Zhang Q, Sun J, et al. High-performance quasi-solid-state flexible aqueous rechargeable Ag–Zn battery based on metal–organic framework-derived ag nanowires. *ACS Energy Lett*. 2018;3:2761-2768.
110. Li H, Peng L, Zhu Y, Zhang X, Yu G. Achieving high-energy–high-power density in a flexible quasi-solid-state sodium ion capacitor. *Nano Lett*. 2016;16:5938-5943.
111. Ming J, Guo J, Xia C, Wang W, Alshareef HN. Zinc-ion batteries: materials, mechanisms, and applications. *Mater Sci Eng R Rep*. 2019;135:58-84.
112. Gong M, Li Y, Zhang H, et al. Ultrafast high-capacity NiZn battery with NiAlCo-layered double hydroxide. *Energy Environ Sci*. 2014;7:2025-2032.
113. Köhler U, Antonius C, Bäuerlein P. Advances in alkaline batteries. *J Power Sources*. 2004;127:45-52.
114. Pan H, Shao Y, Yan P, et al. Reversible aqueous zinc/manganese oxide energy storage from conversion reactions. *Nat Energy*. 2016;1:16039.
115. Cheng FY, Chen J, Gou XL, Shen PW. High-power alkaline Zn–MnO_2 batteries using γ-MnO_2 nanowires/nanotubes and electrolytic zinc powder. *Adv Mater*. 2005;17:2753-2756.
116. Hertzberg BJ, Huang A, Hsieh A, et al. Effect of multiple cation electrolyte mixtures on rechargeable Zn–MnO_2 alkaline battery. *Chem Mater*. 2016;28:4536-4545.
117. Xu C, Li B, Du H, Kang F. Energetic zinc ion chemistry: the rechargeable zinc ion battery. *Angew Chem*. 2012;124:957-959.
118. Yang C-C, Lin S-J. Improvement of high-rate capability of alkaline Zn–MnO_2 battery. *J Power Sources*. 2002;112:174-183.
119. Pasta M, Wessells CD, Huggins RA, Cui Y. A high-rate and long cycle life aqueous electrolyte battery for grid-scale energy storage. *Nat Commun*. 2012;3:1149.
120. Lu Y, Goodenough JB, Kim Y. Aqueous cathode for next-generation alkali-ion batteries. *J Am Chem Soc*. 2011;133:5756-5759.
121. Guan C, Zhao W, Hu Y, et al. High-performance flexible solid-state Ni/Fe battery consisting of metal oxides coated carbon cloth/carbon nanofiber electrodes. *Adv Energy Mater*. 2016;6:1601034.
122. Wang H, Liang Y, Gong M, et al. An ultrafast nickel–iron battery from strongly coupled inorganic nanoparticle/nanocarbon hybrid materials. *Nat Commun*. 2012;3:917.
123. Chakkaravarthy C, Periasamy P, Jegannathan S, Vasu KI. The nickel/iron battery. *J Power Sources*. 1991;35:21-35.
124. Amatucci GG, Badway F, Du Pasquier A, Zheng T. An asymmetric hybrid nonaqueous energy storage cell. *J Electrochem Soc*. 2001;148:A930-A939.
125. Satish R, Aravindan V, Ling WC, Madhavi S. Carbon-coated $Li_3V_2(PO_4)_3$ as insertion type electrode for lithium-ion hybrid electrochemical capacitors: an evaluation of anode and cathodic performance. *J Power Sources*. 2015;281:310-317.

126. Lim E, Jo C, Kim H, et al. Facile synthesis of Nb_2O_5@Carbon core–shell nanocrystals with controlled crystalline structure for high-power anodes in hybrid supercapacitors. *ACS Nano*. 2015;9:7497-7505.
127. Zhang Y, Jing X, Wang Q, Zheng J, Jiang H, Meng C. Three-dimensional porous V_2O_5 hierarchical spheres as a battery-type electrode for a hybrid supercapacitor with excellent charge storage performance. *Dalton Trans*. 2017;46:15048-15058.
128. Hu X, Deng Z, Suo J, Pan Z. A high rate, high capacity and long life ($LiMn_2O_4$+AC)/$Li_4Ti_5O_{12}$ hybrid battery–supercapacitor. *J Power Sources*. 2009;187:635-639.
129. Jiang J, Tan G, Peng S, et al. Electrochemical performance of carbon-coated $Li_3V_2(PO_4)_3$ as a cathode material for asymmetric hybrid capacitors. *Electrochim Acta*. 2013;107:59-65.
130. Li R, Wang Y, Zhou C, et al. Carbon-stabilized high-capacity ferroferric oxide nanorod array for flexible solid-state alkaline battery–supercapacitor hybrid device with high environmental suitability. *Adv Funct Mater*. 2015;25:5384-5394.
131. Wang W, Tang M, Zheng Z, Chen S. Alkaline polymer membrane-based ultrathin, flexible, and high-performance solid-state Zn-Air battery. *Adv Energy Mater*. 2019;9:1803628.
132. Zhou G, Pei S, Li L, et al. A graphene–pure-sulfur sandwich structure for ultrafast, long-life lithium–sulfur batteries. *Adv Mater*. 2014;26:625-631.
133. Ma L, Zhang W, Wang L, et al. Strong capillarity, chemisorption, and electrocatalytic capability of crisscrossed nanostraws enabled flexible, high-rate, and long-cycling lithium–sulfur batteries. *ACS Nano*. 2018;12:4868-4876.
134. Yao M, Wang R, Zhao Z, Liu Y, Niu Z, Chen J. A flexible all-in-one lithium-sulfur battery. *ACS Nano*. 2018;12:12503-12511.
135. Chen X, Liu B, Zhong C, et al. Ultrathin Co_3O_4 layers with large contact area on carbon fibers as high-performance electrode for flexible zinc–air battery integrated with flexible display. *Adv Energy Mater*. 2017;7:1700779.
136. Liu Q-C, Li L, Xu J-J, et al. Flexible and foldable Li–O_2 battery based on paper-ink cathode. *Adv Mater*. 2015;27:8095-8101.
137. Koo M, Park K-I, Lee SH, et al. Bendable inorganic thin-film battery for fully flexible electronic systems. *Nano Lett*. 2012;12:4810-4816.
138. McAlpine MC, Ahmad H, Wang D, Heath JR. Highly ordered nanowire arrays on plastic substrates for ultrasensitive flexible chemical sensors. *Nat Mater*. 2007;6:379-384.
139. Weng Z, Su Y, Wang D-W, Li F, Du J, Cheng HM. Graphene–cellulose paper flexible supercapacitors. *Adv Energy Mater*. 2011;1:917-922.
140. Wu ZS, Parvez K, Feng X, Müllen K. Graphene-based in-plane micro-supercapacitors with high power and energy densities. *Nat Commun*. 2013;4:2487.
141. Feng J-X, Ye S-H, Wang A-L, Lu XF, Tong YX, Li GR. Flexible cellulose paper-based asymmetrical thin film supercapacitors with high-performance for electrochemical energy storage. *Adv Funct Mater*. 2014;24:7093-7101.
142. Chen Y, Cai K, Liu C, Song H, Yang X. High-performance and breathable polypyrrole coated air-laid paper for flexible all-solid-state supercapacitors. *Adv Energy Mater*. 2017;7:1701247.
143. Xue X, Fu Y, Wang Q, Xing L, Zhang Y. Outputting olfactory bionic electric impulse by PANI/PTFE/PANI sandwich nanostructures and their application as flexible, smelling electronic skin. *Adv Funct Mater*. 2016;26:3128-3138.
144. Ren X, Fan H, Zhao Y, Liu Z. Flexible lead-free $BiFeO_3$/PDMS-based nanogenerator as piezoelectric energy harvester. *ACS Appl Mater Interfaces*. 2016;8:26190-26197.
145. Sultana A, Alam MM, Garain S, Sinha TK, Middya TR, Mandal D. An effective electrical throughput from PANI supplement ZnS nanorods and PDMS-based flexible piezoelectric nanogenerator for power up portable electronic devices: an alternative of MWCNT filler. *ACS Appl Mater Interfaces*. 2015;7:19091-19097.
146. Zheng Q, Zhang H, Mi H, Cai Z, Ma Z, Gong S. High-performance flexible piezoelectric nanogenerators consisting of porous cellulose nanofibril (CNF)/poly(dimethylsiloxane) (PDMS) aerogel films. *Nano Energy*. 2016;26:504-512.
147. Lee J, Wu J, Shi M, et al. Stretchable GaAs photovoltaics with designs that enable high areal coverage. *Adv Mater*. 2011;23:986-991.
148. Koh A, Kang D, Xue Y, et al. A soft, wearable microfluidic device for the capture, storage, and colorimetric sensing of sweat. *Sci Transl Med*. 2016;8:366ra165.
149. Kim D-H, Lu N, Ma R, et al. Epidermal electronics. *Science*. 2011;333:838-843.
150. Kim J, Lee M, Shim HJ, et al. Stretchable silicon nanoribbon electronics for skin prosthesis. *Nat Commun*. 2014;5:5747.
151. Mannsfeld SCB, Tee BCK, Stoltenberg RM, et al. Highly sensitive flexible pressure sensors with microstructured rubber dielectric layers. *Nat Mater*. 2010;9:859-864.
152. Zirkl M, Haase A, Fian A, et al. Low-voltage organic thin-film transistors with high-k nanocomposite gate dielectrics for flexible electronics and optothermal sensors. *Adv Mater*. 2007;19:2241-2245.
153. Liu X, Miao J, Fan Q, et al. Recent progress on smart fiber and textile based wearable strain sensors: materials, fabrications and applications. *Adv Fiber Mater*. 2022;4:361-389.
154. Chen Z, Ren W, Gao L, Liu B, Pei S, Cheng HM. Three-dimensional flexible and conductive interconnected graphene networks grown by chemical vapour deposition. *Nat Mater*. 2011;10:424-428.
155. Chen Z, Xu C, Ma C, Ren W, Cheng HM. Lightweight and flexible graphene foam composites for high-performance electromagnetic interference shielding. *Adv Mater*. 2013;25:1296-1300.
156. Chen B, Tang W, Jiang T, et al. Three-dimensional ultraflexible triboelectric nanogenerator made by 3D printing. *Nano Energy*. 2018;45:380-389.
157. Wu C, Park JH, Koo B, Chen X, Wang ZL, Kim TW. Capsule triboelectric nanogenerators: toward optional 3D integration for high output and efficient energy harvesting from broadband-amplitude vibrations. *ACS Nano*. 2018;12:9947-9957.
158. Qi Z, Ye J, Chen W, et al. 3D-printed, superelastic polypyrrole–graphene electrodes with ultrahigh areal capacitance for electrochemical energy storage. *Adv. Mater. Technol.* 2018;3:1800053.
159. Chen G, Rastak R, Wang Y, et al. Strain- and strain-rate-invariant conductance in a stretchable and compressible 3D conducting polymer foam. *Matter*. 2019;1:205-218.
160. Xu Y, Lin Z, Huang X, Liu Y, Huang Y, Duan X. Flexible solid-state supercapacitors based on three-dimensional graphene hydrogel films. *ACS Nano*. 2013;7:4042-4049.

161. Zhao Y, Liu J, Hu Y, et al. Highly compression-tolerant supercapacitor based on polypyrrole-mediated graphene foam electrodes. *Adv Mater*. 2013;25:591-595.
162. Zhang X, Lin Z, Chen B, et al. Solid-state flexible polyaniline/silver cellulose nanofibrils aerogel supercapacitors. *J Power Sources*. 2014;246:283-289.
163. Tang Z, Gao L, Wu Y, et al. BSA–rGO nanocomposite hydrogel formed by UV polymerization and in situ reduction applied as biosensor electrode. *J Mater Chem B*. 2013;1:5393-5397.
164. Han L, Lu X, Wang M, et al. A mussel-inspired conductive, self-adhesive, and self-healable tough hydrogel as cell stimulators and implantable bioelectronics. *Small*. 2017;13:1601916.
165. Salvatore GA, Münzenrieder N, Kinkeldei T, et al. Wafer-scale design of lightweight and transparent electronics that wraps around hairs. *Nat Commun*. 2014;5:2982.
166. Harada S, Kanao K, Yamamoto Y, Arie T, Akita S, Takei K. Fully printed flexible fingerprint-like three-axis tactile and slip force and temperature sensors for artificial skin. *ACS Nano*. 2014;8:12851-12857.
167. Jin X, Song L, Yang H, et al. Stretchable supercapacitor at −30°C. *Energy Environ Sci*. 2021;14:3075-3085.
168. Wang ZL, Song J. Piezoelectric nanogenerators based on zinc oxide nanowire arrays. *Science*. 2006;312:242-246.
169. Park K-I, Son JH, Hwang G-T, et al. Highly-efficient, flexible piezoelectric PZT thin film nanogenerator on plastic substrates. *Adv Mater*. 2014;26:2514-2520.
170. Lin L, Wang S, Xie Y, et al. Segmentally structured disk triboelectric nanogenerator for harvesting rotational mechanical energy. *Nano Lett*. 2013;13:2916-2923.
171. Yang Y, Guo W, Pradel KC, et al. Pyroelectric nanogenerators for harvesting thermoelectric energy. *Nano Lett*. 2012;12:2833-2838.
172. Zeng W, Shu L, Li Q, Chen S, Wang F, Tao XM. Fiber-based wearable electronics: a review of materials, fabrication, devices, and applications. *Adv Mater*. 2014;26:5310-5336.
173. Qi Y, McAlpine MC. Nanotechnology-enabled flexible and biocompatible energy harvesting. *Energy Environ Sci*. 2010;3:1275-1285.
174. Wang ZL. Towards self-powered nanosystems: from nanogenerators to nanopiezotronics. *Adv Funct Mater*. 2008;18:3553-3567.
175. Wang X, Song J, Liu J, Wang ZL. Direct-current nanogenerator driven by ultrasonic waves. *Science*. 2007;316:102-105.
176. Gao PX, Song J, Liu J, Wang ZL. Nanowire piezoelectric nanogenerators on plastic substrates as flexible power sources for nanodevices. *Adv Mater*. 2007;19:67-72.
177. Donelan JM, Li Q, Naing V, Hoffer JA, Weber DJ, Kuo AD. Biomechanical energy harvesting: generating electricity during walking with minimal user effort. *Science*. 2008;319:807-810.
178. Angell CA, Liu C, Sanchez E. Rubbery solid electrolytes with dominant cationic transport and high ambient conductivity. *Nature*. 1993;362:137-139.
179. Huang Y, Zhong M, Huang Y, et al. A self-healable and highly stretchable supercapacitor based on a dual crosslinked polyelectrolyte. *Nat Commun*. 2015;6:10310.
180. Ma Q, Zhang H, Zhou C, et al. Single lithium-ion conducting polymer electrolytes based on a super-delocalized polyanion. *Angew Chem, Int Ed*. 2016;55:2521-2525.
181. Wan J, Xie J, Kong X, et al. Ultrathin, flexible, solid polymer composite electrolyte enabled with aligned nanoporous host for lithium batteries. *Nat Nanotechnol*. 2019;14:705-711.
182. Chen L, Li Y, Li S-P, Fan LZ, Nan CW, Goodenough JB. PEO/garnet composite electrolytes for solid-state lithium batteries: from "ceramic-in-polymer" to "polymer-in-ceramic". *Nano Energy*. 2018;46:176-184.
183. Feng S, Shi D, Liu F, et al. Single lithium-ion conducting polymer electrolytes based on poly[(4-styrenesulfonyl)(trifluoromethanesulfonyl)imide] anions. *Electrochim Acta*. 2013;93:254-263.
184. Ha H-J, Kil E-H, Kwon YH, Kim JY, Lee CK, Lee SY. UV-curable semi-interpenetrating polymer network-integrated, highly bendable plastic crystal composite electrolytes for shape-conformable all-solid-state lithium ion batteries. *Energy Environ Sci*. 2012;5:6491-6499.
185. Wei D, Haque S, Andrew P, et al. Ultrathin rechargeable all-solid-state batteries based on monolayer graphene. *J Mater Chem A*. 2013;1:3177-3181.
186. Rohan R, Pareek K, Cai W, et al. Melamine–terephthalaldehyde–lithium complex: a porous organic network based single ion electrolyte for lithium ion batteries. *J Mater Chem A*. 2015;3:5132-5139.
187. Saricilar (Zengin) S, Antiohos D, Shu K, et al. High strain stretchable solid electrolytes. *Electrochem Commun*. 2013;32:47-50.
188. Kadokawa, J, Egashira N, Yamamoto K. Chemoenzymatic preparation of amylose-grafted chitin nanofiber network materials. *Biomacromolecules*. 2018;19:3013-3019.
189. Yu H, Wu J, Fan L, et al. A novel redox-mediated gel polymer electrolyte for high-performance supercapacitor. *J Power Sources*. 2012;198:402-407.
190. Zhao C, Wang C, Yue Z, Shu K, Wallace GG. Intrinsically stretchable supercapacitors composed of polypyrrole electrodes and highly stretchable gel electrolyte. *ACS Appl Mater Interfaces*. 2013;5:9008-9014.
191. Cheng EJ, Kimura T, Shoji M, Ueda H, Munakata H, Kanamura K. Ceramic-based flexible sheet electrolyte for Li batteries. *ACS Appl Mater Interfaces*. 2020;12:10382-10388.
192. Jiang T, He P, Wang G, Shen Y, Nan CW, Fan LZ. Solvent-free synthesis of thin, flexible, nonflammable garnet-based composite solid electrolyte for all-solid-state lithium batteries. *Adv Energy Mater*. 2020;10:1903376.
193. Jacob MME, Hackett E, Giannelis EP. From nanocomposite to nanogel polymer electrolytes. *J Mater Chem*. 2003;13:1-5.
194. Liu W, Liu N, Sun J, et al. Ionic conductivity enhancement of polymer electrolytes with ceramic nanowire fillers. *Nano Lett*. 2015;15:2740-2745.
195. Zheng J, Tang M, Hu Y-Y. Lithium ion pathway within $Li_7La_3Zr_2O_{12}$-polyethylene oxide composite electrolytes. *Angew Chem, Int Ed*. 2016;55:12538-12542.
196. Zhou W, Wang S, Li Y, Xin S, Manthiram A, Goodenough JB. Plating a dendrite-free lithium anode with a polymer/ceramic/polymer sandwich electrolyte. *J Am Chem Soc*. 2016;138:9385-9388.
197. Wang Z, Pan R, Sun R, Edström K, Strømme M, Nyholm L. Nanocellulose structured paper-based lithium metal batteries. *ACS Appl Energy Mater*. 2018;1:4341-4350.

198. Liu J, Qian T, Wang M, Zhou J, Xu N, Yan C. Use of tween polymer to enhance the compatibility of the Li/electrolyte interface for the high-performance and high-safety quasi-solid-state lithium–sulfur battery. *Nano Lett*. 2018;18:4598-4605.
199. Zhang D, Xu X, Huang X, et al. A flexible composite solid electrolyte with a highly stable interphase for dendrite-free and durable all-solid-state lithium metal batteries. *J Mater Chem A*. 2020;8:18043-18054.
200. Huo H, Chen Y, Luo J, Yang X, Guo X, Sun X. Rational design of hierarchical "Ceramic-in-Polymer" and "Polymer-in-Ceramic" electrolytes for dendrite-free solid-state batteries. *Adv Energy Mater*. 2019;9:1804004.
201. Zhang W, Miao J, Tian M, Zhang X, Fan T, Qu L. Hierarchically interlocked helical conductive yarn enables ultra-stretchable electronics and smart fabrics. *Chem Eng J*. 2023;462:142279.
202. Shi Y, Pan L, Liu B, et al. Nanostructured conductive polypyrrole hydrogels as high-performance, flexible supercapacitor electrodes. *J Mater Chem A*. 2014;2:6086-6091.

AUTHOR BIOGRAPHIES

Qi Zhang is a lecturer in Engineering Research Center of Advanced Metal Composites Forming Technology and Equipment, Taiyuan University of Technology. His current research interest is high value-added utilization of biomass, renewable energy storage and conversion and the corrosion resistance of metal composite.

Wen-Bin Luo is a full-time professor at Northeastern University (Shenyang, China) and Director of Institute for Energy Electrochemistry and Urban Mines Metallurgy. He is a honored as a National Young Talent and LiaoNing Revitalization Talent. He obtained his Bachelor's and Master's degrees from Northeastern University in 2009 and 2011, respectively, and completed his PhD at the University of Wollongong (Australia) in 2015. His research focuses on energy conversion and storage materials and urban mines metallurgy.

How to cite this article: Zhang Q, Gao X-W, Liu X, et al. Flexible wearable energy storage devices: materials, structures, and applications. *Battery Energy*. 2024;3:20230061. doi:10.1002/bte2.20230061